Cobalt(II) Triazene 1-Oxide Bis(chelates). A Case of Planar (Low Spin)–Tetrahedral (High Spin) Isomerism†

Juliusz A. Wolny, Mikołaj F. Rudolf,* Zbigniew Ciunik, Kazimierz Gatner and Stanisław Wołowiec
*Institute of Chemistry, University of Wrocław, Joliot-Curie 14, 50-383 Wrocław, Poland*

High- and low-spin cobalt(II) triazene 1-oxide bis(chelates) have been isolated. The low-spin complexes possess square-planar structure whilst the high-spin complexes are tetrahedral. The molecular structure of high-spin $[Co(OMeN_3C_6H_4Me-4)_2]$ has been determined: triclinic, space group $P\bar{1}$, $Z = 2$, $a = 7.970(5)$, $b = 10.174(5)$, $c = 11.676(5)$ Å, $\alpha = 87.18(4)$, $\beta = 74.31(4)$ and $\gamma = 74.06(4)°$. For some complexes the isolation of both planar (low-spin) and tetrahedral (high-spin) isomers or of their conglomerates is possible depending on the synthesis conditions. The crystal structure of square-planar $[Ni(OMeN_3C_6H_4-Me-4)_2]$, which is isomorphous with the low-spin isomer of $[Co(OMeN_3C_6H_4Me-4)_2]$, has been determined: triclinic, space group $P\bar{1}$, $Z = 1$, with $a = 7.495(2)$, $b = 7.694(5)$, $c = 8.612(3)$ Å, $\alpha = 64.64(5)$, $\beta = 87.84(2)$ and $\gamma = 78.64(3)°$. The complexes exhibit a planar–tetrahedral equilibrium in non-co-ordinating solvents, the $\Delta H^\ominus$ and $\Delta S^\ominus$ values of which, determined from solution magnetic susceptibility measurements, are in the range $1–15$ kJ mol^{-1} and $5–30$ J K^{-1} mol^{-1}, respectively. The electrochemical properties of the complexes are given.

The first report on metal complexes of triazene 1-oxides appeared as early as in 1938.[1] Since that time some interest has centred around the formation and properties of these compounds.[2] The synthesis of the ligands is quite straightforward and involves coupling the diazotised aromatic amines and *N*-alkyl- or aryl-hydroxylamines, the latter prepared by reduction of the corresponding nitro compounds. A host of differently substituted starting materials is available. Hence it is possible to introduce into a ligand system a number of substituents of different size and polar effects. In a previous communication[2j] we reported the formation of both high- and low-spin cobalt(II) complexes, the spin state being dependent on the ligand substituents. The structure of low-spin $[Co(OEtN_3Ph)_2]$ was shown to be square-planar centrosymmetric.[2j] The formation of low-spin bis(chelate) cobalt(II) systems with an N_2O_2 chromophore indicates rather strong σ-donor properties of triazen-1-olato anions. We also pointed out the possibility of conversion of some of the high-spin complexes into low-spin isomers upon dissolution in non-co-ordinating solvents or by recrystallisation from dimethylformamide (dmf)–water.

This paper describes the isolation, magnetic, electrochemical and spectroscopic properties of cobalt(II) chelates of systematically substituted triazene 1-oxides. The molecular structure of high-spin, tetrahedral $[Co(OMeN_3C_6H_4Me-4)_2]$ has been determined. The formation of high- and low-spin complexes and their interconversions have been found to be due to tetrahedral–planar isomerism. This phenomenon is well documented for four-co-ordinate nickel(II) bis(chelates)[3] but is very scarce for analogous cobalt(II) systems.[4]

Experimental

Details of the magnetic, spectroscopic and electrochemical instrumentation are given in refs. 2(*k*) and 2(*n*). Magnetic susceptibility measurements in $CDCl_3$ and $C_6D_5CD_3$ solutions were performed by means of the Evans method[5] using a Bruker AMX 300 NMR spectrometer. Diffuse reflectance spectra were measured on a Cary 5 spectrometer with MgO as standard, FIR spectra on a Perkin Elmer 180 spectrometer. The synthesis of

[Co(ORN₃C₆HₙX)₂]
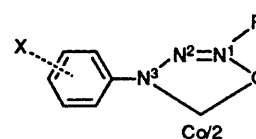
R = Me, Et, Pr^n, Bu^t or Ph

X = 4-H, 4-Me, 4-Et, 4-Pr^n, 4-Bu^n, 4-OMe, 4-Cl, 4-Br, 4-CO₂Et, 4-NO₂, 3-Me, 2-Me, 2, 4-Me₂, 2,5-Me₂, 2,6-Me₂, 2,3-Me₂, or 2-Me-4-NO₂

$n = 3$ or 4

the complexes, the electrochemical and spectroscopic measurements were all performed under an inert atmosphere of purified (BTS catalyst, 4 Å molecular sieves) dinitrogen or argon.

Materials and Ligand Preparations.—Organic solvents were purified and dried using literature methods.[6] *N*-Substituted hydroxylamines were obtained from the corresponding nitroalkanes by means of reduction with zinc.[7] Aromatic amines were diazotised by means of literature methods.[8] The ligands were synthesised according to the method of Bamberger and Renauld.[9] A typical synthesis, namely that of 4-ClC₆H₄N₃-MeOH, is given in ref. 2(*k*). The crude solid products obtained were recrystallised with charcoal. The following solvents were used (crystallisation yield in parentheses): light petroleum (b.p. 40–60 °C) for 2-MeC₆H₄N₃MeOH (50), 3-MeC₆H₄N₃MeOH (60), 4-EtC₆H₄N₃MeOH (65), 4-Pr^{n}C₆H₄N₃MeOH (70), 4-Bu^{n}C₆H₄N₃MeOH (60), 2,4-Me₂C₆H₃N₃MeOH (50), 2,5-Me₂C₆H₃N₃MeOH (50), 2,3-Me₂C₆H₃N₃EtOH (60), 2,5-Me₂C₆H₃N₃EtOH (40), 4-MeC₆H₄N₃EtOH (50), PhN₃Bu^{t}OH (50), 2,6-Me₂C₆H₃N₃EtOH (60%), 4-MeC₆H₄N₃Bu^{t}OH (80), 3-MeC₆H₄N₃Bu^{t}OH (65), 2,3-Me₂C₆H₃N₃Bu^{t}OH (60), 2,6-Me₂C₆H₃N₃Bu^{t}OH (60), 3-MeC₆H₄N₃EtOH (40), 4-MeOC₆-H₄N₃Bu^{t}OH (30), PhN₃Pr^{n}OH (70), 2-MeC₆H₄N₃Pr^{n}OH (60), 3-MeC₆H₄N₃Pr^{n}OH (65), 4-MeC₆H₄N₃Pr^{n}OH (70), 4-Cl-C₆H₄N₃Pr^{n}OH (80), 4-BrC₆H₄N₃Pr^{n}OH (75), 2,6-Me₂C₆H₃-N₃Pr^{n}OH (60), 2,4-Me₂C₆H₃N₃Pr^{n}OH (50), 2,4-Me₂C₆H₃-N₃Pr^{n}OH (55); light petroleum–benzene (30 : 1) for PhN₃MeOH (30, double crystallisation); light petroleum–benzene (8 : 1) for

4-MeC$_6$H$_4$N$_3$MeOH (60); light petroleum–benzene (6:1) for 3-MeC$_6$H$_4$N$_3$EtOH (50), 4-OMeC$_6$H$_4$N$_3$EtOH (45), 4-OMeC$_6$H$_4$N$_3$MeOH (50); light petroleum–benzene (2:1) for PhN$_3$EtOH (55); light petroleum–benzene (1:1) for 4-ClC$_6$H$_4$-N$_3$MeOH (40), 4-BrC$_6$H$_4$N$_3$MeOH (40), 4-ClC$_6$H$_4$N$_3$EtOH (50), 4-BrC$_6$H$_4$N$_3$EtOH; methanol for 2-Me-4-NO$_2$C$_6$H$_3$N$_3$-MeOH (40), 4-EtCO$_2$C$_6$H$_4$N$_3$MeOH (60), 4-ClC$_6$H$_4$N$_3$Bu^{t}OH (85), 4-BrC$_6$H$_4$N$_3$Bu^{t}OH (80), 4-EtCO$_2$C$_6$H$_4$N$_3$Bu^{t}OH (70), 4-NO$_2$C$_6$H$_4$N$_3$Bu^{t}OH (40), 4-NO$_2$C$_6$H$_4$N$_3$Pr^{n}OH (65), 2-Me-4-NO$_2$C$_6$H$_3$N$_3$Pr^{n}OH (50), PhN$_3$PhOH (60), 4-MeC$_6$H$_4$N$_3$-PhOH (55), 4-BrC$_6$H$_4$N$_3$PhOH (70), 4-EtCO$_2$C$_6$H$_4$N$_3$PhOH (45); ethanol for 2,3-Me$_2$C$_6$H$_3$N$_3$MeOH (70); toluene for 4-NO$_2$C$_6$H$_4$N$_3$EtOH (60); and pyridine for 4-NO$_2$C$_6$H$_4$N$_3$-MeOH (80). In a few cases, *i.e.* for 2,6-Me$_2$C$_6$H$_3$N$_3$MeOH, 2-MeC$_6$H$_4$N$_3$EtOH, 2,4-Me$_2$C$_6$H$_3$N$_3$EtOH, 2-MeC$_6$H$_4$N$_3$-Bu^{t}OH and 2,4-Me$_2$C$_6$H$_3$N$_3$Bu^{t}OH, the synthesis yielded oily products which were extracted with diethyl ether, the ether layer being dried over anhydrous magnesium sulfate, boiled with charcoal and filtered. After removal of the solvent the semisolid ligands obtained were used for the synthesis of complexes without further purification.

Preparation of Complexes.—The usual procedure involved direct reaction between the ligand and cobalt(II) acetate tetrahydrate. Typically, the ligand (5 mmol) was dissolved in the minimum volume of boiling methanol in an inert atmosphere. The volume is dependent on the ligand and varied from 5 cm^3 for PhN$_3$MeOH to 90 cm^3 for 4-NO$_2$C$_6$H$_4$N$_3$EtOH. A solution of Co(O$_2$CMe)$_2$·4H$_2$O (2.5 mmol) in degassed methanol (10 cm^3) was then added dropwise. Depending on the ligand, the complex was either deposited immediately {*e.g.* for [Co(OMeN$_3$C$_6$H$_4$X-4)$_2$], X = Me, Cl or Br} or upon cooling. The complex was then filtered off, washed with cooled, degassed methanol and dried *in vacuo*. The solvent volumes used for syntheses and the results of elemental analysis together with magnetic moments at 77 and 293 K are collected in Table 1.

Syntheses at low temperatures. For [Co(OMeC$_6$H$_4$N$_3$Me-4)$_2$] a series of syntheses were performed at −13, 10, 20, 30 and at 63 °C (boiling methanol). The ligand (0.825 g, 5 mmol) was added to degassed MeOH (16 cm^3) and heated or cooled to a given temperature. At lower temperatures the reaction proceeded with the presence of some partly suspended ligand. Then a degassed solution of Co(O$_2$CMe)$_2$·4H$_2$O (2.5 mmol) in MeOH (12 cm^3) was added dropwise, slowly enough to keep the temperature of the reaction mixture constant. The resulting precipitates were filtered off quickly, washed with cool methanol and dried *in vacuo*. In all cases the results of elemental analysis fitted the calculated values.

For three complexes, *i.e.* [Co(OMeN$_3$Ph)$_2$], [Co(OMeN$_3$-C$_6$H$_4$Cl-4)$_2$] and [Co(OMeN$_3$C$_6$H$_4$Me-3)$_2$], syntheses at *ca.* −60 °C were carried out under anaerobic conditions using double-walled, thermostatted (Pr^{i}OH–solid CO$_2$ bath) Schlenk-type glassware.

[Co(OMeN$_3$C$_6$H$_4$Me-3)$_2$]. The ligand (5 mmol) was dissolved in MeOH (8 cm^3) and placed in a thermostatted Schlenk apparatus. Triethylamine (5 mmol) was then added and after deoxygenation for 10 min a cooled, degassed solution of Co(O$_2$CMe)$_2$·4H$_2$O (2.5 mmol) in MeOH (8 cm^3) was added dropwise. After 2 h the resulting, crystalline precipitate was filtered off at −50 °C, washed with MeOH (10 cm^3) cooled to −50 °C and dried in a stream of cold argon [Found (Calc.): C, 49.3 (49.6); H, 5.3 (5.2); N, 21.7 (21.7%)].

[Co(OMeN$_3$Ph)$_2$]. The salt Co(O$_2$CMe)$_2$·4H$_2$O (2.5 mmol) was dissolved in MeOH (7 cm^3), placed in a thermostatted Schlenk apparatus and deoxygenated in a stream of argon. A cooled, degassed solution of ligand (5 mmol) and triethylamine (5 mmol) in MeOH (8 cm^3) was added dropwise. After 2 h, cooled, degassed hexane (10 cm^3) was added resulting in the deposition of a yellow precipitate, which was filtered off and dried in a stream of cool argon. The precipitate darkened upon drying [Found (Calc.): C, 47.0 (46.8); H, 4.6 (4.5); N, 23.4 (23.4%)].

[Co(OMeN$_3$C$_6$H$_4$Cl-4)$_2$]. The ligand (5 mmol) was suspended in MeOH (80 cm^3) in a thermostatted Schlenk apparatus and triethylamine (5 mmol) added. The resulting suspension was deoxygenated in a stream of argon. A cooled, degassed solution of Co(O$_2$CMe)$_2$·4H$_2$O (2.5 mmol) was added dropwise. After 3 h of bubbling with argon a brown precipitate deposited which was filtered off, washed with cooled, degassed methanol and dried in a stream of argon. In the course of drying the complex became dark red [Found (Calc.): C, 39.6 (39.3); H, 3.3 (3.3); Cl, 16.4 (16.6); N, 20.0 (19.6%)].

The four complexes [Co(OMeN$_3$C$_6$H$_4$Me-4)$_2$], [Co(OMe-N$_3$C$_6$H$_4$Cl-4)$_2$], [Co(OMeN$_3$C$_6$H$_4$Br-4)$_2$] and [Co(OMe-N$_3$Ph)$_2$] were precipitated from dmf solutions. In a typical procedure the high-spin complex obtained by synthesis in boiling MeOH was dissolved in dmf under anaerobic conditions and precipitated by the dropwise addition of an equal volume of degassed water over a period of 3 h. The resulting precipitates were filtered off, washed with water and dried *in vacuo* over P$_4$O$_{10}$. The analytical data and the conditions of precipitation are summarised in Table 2.

The bis(chelate) complexes studied are stable in air but undergo oxidation in solution, quite rapidly for those bearing unsubstituted, alkyl- or methoxy-substituted phenyl rings on the ligands. They decompose when heated to temperatures above 120 °C, in some cases violently.

Single crystals of [Ni(OMeN$_3$C$_6$H$_4$Me-4)$_2$] were grown from dichloromethane. This complex was prepared as described. Single crystals of high-spin [Co(OMeN$_3$C$_6$H$_4$Me-4)$_2$] were grown under anaerobic conditions by slow diffusion of a methanolic solution of Co(O$_2$CMe)$_2$·4H$_2$O into a benzene solution of ligand in a sealed glass tube of 4 mm diameter with a capillary narrowing.

Crystal-structure Determinations of [Ni(OMeN$_3$C$_6$H$_4$Me-4)$_2$] *and High-spin* [Co(OMeN$_3$C$_6$H$_4$Me-4)$_2$].—*High-spin* [Co(OMeN$_3$C$_6$H$_4$Me-4)$_2$]. *Crystal data.* C$_{16}$H$_{20}$CoN$_6$O$_2$, $M = 387.35$, red plates, crystal dimensions 0.4 × 0.4 × 0.5 mm, triclinic, space group $P\bar{1}$, $a = 7.970(5)$, $b = 10.174(5)$, $c = 11.676(5)$ Å, $\alpha = 87.18(4)$, $\beta = 74.31(4)$, $\gamma = 74.06(4)°$, $U = 876.1(8)$ Å^3 (by least-squares refinement of diffractometer angles for 15 automatically centred reflections), $D_c = 1.468(1)$ g cm^{-3}, $Z = 2$, μ(Mo-Kα) = 10.4 cm^{-1}, $F(000) = 402$.

3082 Independent reflections up to $2\theta = 50°$ were measured on a Syntex P2$_1$ diffractometer with graphite-monochromated Mo-Kα radiation using the ω–2θ scan mode. 2737 Reflections were considered as observed [$I > 1.96\sigma(I)$]. Two standard reflections showed no variation. Data were corrected for Lorentz, polarisation and absorption effects (DIFABS program [10]). Correction coefficients were in the range 0.734–1.220. The structure was solved using Patterson and Fourier techniques. Most H atoms were found on a difference map; the others were located at the calculated positions (C–H 0.95 Å). Full-matrix least-squares refinement of 226 non-H atom (H-atom parameters were fixed) converged at $R = 0.041$, $R' = 0.046$ [$w = \sigma^{-2}(F)$]; final $(\Delta/\sigma)_{max} = 0.25$; $-0.22 < \Delta\rho < 0.35$ e Å^{-3} in final ΔF map. All crystallographic computations were performed with use of XTL/XTLE programs [11] with neutral-atom scattering factors as included in the program.

[Ni(OMeN$_3$C$_6$H$_4$Me-4)$_2$]. *Crystal data.* C$_{16}$H$_{20}$N$_6$NiO$_2$, $M = 387.09$, green cubes, crystal dimensions 0.25 × 0.30 × 0.30 mm, triclinic, space group $P\bar{1}$, $a = 7.495(2)$, $b = 7.694(5)$, $c = 8.612(3)$ Å, $\alpha = 64.64(5)$, $\beta = 87.84(2)$, $\gamma = 78.64(3)$, $U = 439.4(4)$ Å^3 (by least-squares refinements of diffractometer angles for 25 automatically centred reflections), $D_c = 1.463(1)$ g cm^{-3}, $Z = 1$, μ(Mo-Kα) = 10.64 cm^{-1}, $F(000) = 202$.

1662 Reflections up to $2\theta = 50°$ (1509 independent) were measured on a Kuma KM4 k-axis diffractometer with graphite-monochromated Mo-Kα radiation using the ω–2θ scan mode. 1400 Reflections were considered as observed [$I > 3\sigma(I)$]. Three standard reflections showed no variation. Data were corrected for Lorentz and polarisation effects, but not for

Table 1 Preparation conditions (synthesis in boiling methanol), elemental analysis[a] and magnetic characterisation of the cobalt(II) chelates

		Analysis (%)				μ	
Chelate	V^b/cm^3	C	H	N	X	77	293 K
[Co(OMeN$_3$Ph)$_2$]	4	46.9 (46.8)	4.4 (4.5)	23.5 (23.4)		5.15	5.24
[Co(OMeN$_3$C$_6$H$_4$Me-2)$_2$]	10	49.4 (49.6)	4.9 (5.2)	21.6 (21.7)		1.92	1.94
[Co(OMeN$_3$C$_6$H$_4$Me-4)$_2$]	15	49.6 (49.6)	5.2 (5.2)	21.9 (21.7)		5.15	4.88
[Co(OMeN$_3$C$_6$H$_4$Me-3)$_2$]	10 + 10^c	49.8 (49.6)	5.0 (5.2)	21.9 (21.7)		4.94	4.83
[Co(OMeN$_3$C$_6$H$_4$Cl-4)$_2$]	15	39.4 (39.3)	3.5 (3.3)	19.7 (19.6)	16.5 (16.6)	4.77	4.49
[Co(OMeN$_3$C$_6$H$_4$Br-4)$_2$]	15	32.1 (32.5)	2.7 (2.7)	16.0 (16.2)	31.1 (30.9)	4.78	4.68
[Co(OMeN$_3$C$_6$H$_4$CO$_2$Et-4)$_2$]	20^d	47.9 (47.7)	4.6 (4.8)	16.3 (16.7)		4.40	4.30
[Co(OMeN$_3$C$_6$H$_4$NO$_2$-4)$_2$]	25^e	37.3 (37.4)	2.9 (3.1)	25.6 (24.9)		4.66	4.64
[Co(OMeN$_3$C$_6$H$_3$Me-2-NO$_2$-4)$_2$]	50	40.4 (40.3)	3.8 (3.8)	23.5 (23.5)		1.90	2.09
[Co(OMeN$_3$C$_6$H$_3$Me-3-NO$_2$-4)$_2$]	50	40.3 (40.3)	3.8 (3.8)	23.5 (23.5)		5.07	5.11
[Co(OEtN$_3$C$_6$H$_3$Me$_2$-2,4)$_2$]	10	54.2 (54.2)	6.3 (6.3)	18.8 (19.0)		2.09	2.06
[Co(OEtN$_3$C$_6$H$_3$Me$_2$-2,3)$_2$]	10	54.5 (54.2)	6.4 (6.3)	18.7 (19.0)		2.02	2.03
[Co(OEtN$_3$C$_6$H$_3$Me$_2$-2,6)$_2$]	10	54.5 (54.2)	6.7 (6.3)	18.8 (19.0)		2.04	2.05
[Co(OEtN$_3$C$_6$H$_3$Me$_2$-2,5)$_2$]	10	54.2 (54.2)	6.6 (6.3)	19.0 (19.0)		1.90	1.95
[Co(OMeN$_3$C$_6$H$_4$OMe-4)$_2$]	10	45.6 (45.8)	5.0 (4.8)	19.9 (20.0)		1.96	1.90
[Co(OMeN$_3$C$_6$H$_4$Et-4)$_2$]	10	52.1 (52.1)	5.7 (5.8)	20.4 (20.2)		4.78	4.78
[Co(OMeN$_3$C$_6$H$_4$Pr^n-4)$_2$]	8	54.3 (54.2)	6.2 (6.3)	19.1 (19.0)		1.90	1.96
[Co(OMeN$_3$C$_6$H$_4$Bu^n-4)$_2$]	10	56.1 (56.1)	6.9 (6.8)	17.6 (17.8)		1.92	2.00
[Co(OEtN$_3$Ph)$_2$]	4	49.7 (49.6)	5.2 (5.2)	21.9 (21.7)		1.90	2.08
[Co(OEtN$_3$C$_6$H$_4$Me-2)$_2$]	6	51.7 (52.1)	5.3 (5.8)	19.9 (20.2)		1.90	1.90
[Co(OEtN$_3$C$_6$H$_4$Me-4)$_2$]	8	52.5 (52.1)	5.4 (5.8)	20.3 (20.2)		1.99	2.03
[Co(OEtN$_3$C$_6$H$_4$Cl-4)$_2$]	8	42.1 (42.1)	4.0 (3.9)	18.3 (18.4)	15.5 (15.5)	1.90	1.97
[Co(OEtN$_3$C$_6$H$_4$Br-4)$_2$]	8	35.2 (35.3)	3.2 (3.3)	15.3 (15.4)	29.2 (29.3)	1.93	1.98
[Co(OEtN$_3$C$_6$H$_4$NO$_2$-4)$_2$]	90	40.0 (40.3)	3.6 (3.8)	24.0 (23.5)		4.97	4.99
[Co(OEtN$_3$C$_6$H$_4$OMe-4)$_2$]	8	48.1 (48.3)	5.4 (5.4)	18.6 (18.8)		2.12	2.12
[Co(OMeN$_3$C$_6$H$_3$Me$_2$-2,6)$_2$]	10	51.1 (52.1)	6.0 (5.8)	19.5 (20.2)		1.90	1.90
[Co(OMeN$_3$C$_6$H$_3$Me$_2$-2,5)$_2$]	10	52.1 (52.1)	5.6 (5.8)	20.5 (20.2)		2.04	1.95
[Co(OMeN$_3$C$_6$H$_3$Me$_2$-2,4)$_2$]	10	51.8 (52.1)	5.7 (5.8)	19.9 (20.2)		2.07	2.04
[Co(OMeN$_3$C$_6$H$_3$Me$_2$-2,3)$_2$]	10	51.7 (52.1)	5.7 (5.8)	19.8 (20.2)		1.98	1.90
[Co(OBu^{t}N$_3$Ph)$_2$]	5	54.3 (54.2)	6.3 (6.3)	18.8 (19.0)		2.06	2.09
[Co(OBu^{t}N$_3$C$_6$H$_4$OMe-4)$_2$]	10	52.8 (52.9)	5.5 (5.6)	16.8 (16.8)		2.02	2.03
[Co(OBu^{t}N$_3$C$_6$H$_4$Me-4)$_2$]	5	56.3 (56.1)	6.9 (6.8)	18.1 (17.8)		2.01	2.00
[Co(OBu^{t}N$_3$C$_6$H$_4$Me-2)$_2$]	5	56.2 (56.1)	6.9 (6.8)	18.6 (17.8)		1.90	1.93
[Co(OBu^{t}N$_3$C$_6$H$_4$Cl-4)$_2$]	5	46.7 (46.9)	5.0 (5.1)	16.3 (16.4)	13.9 (13.9)	1.96	1.90
[Co(OBu^{t}N$_3$C$_6$H$_4$Br-4)$_2$]	5	40.0 (40.0)	4.2 (4.3)	13.8 (14.0)	26.7 (26.6)	2.06	2.07
[Co(OBu^{t}N$_3$C$_6$H$_3$Me$_2$-2,6)$_2$]	5	58.1 (57.7)	7.5 (7.2)	16.5 (16.8)		1.90	1.90
[Co(OBu^{t}N$_3$C$_6$H$_3$Me$_2$-2,4)$_2$]	5	57.3 (57.7)	7.5 (7.2)	16.6 (16.8)		1.92	1.96
[Co(OBu^{t}N$_3$C$_6$H$_3$Me$_2$-2,3)$_2$]	5	57.4 (57.7)	7.5 (7.2)	16.2 (16.8)		1.94	1.90
[Co(OBu^{t}N$_3$C$_6$H$_4$CO$_2$Et-4)$_2$]	8	56.2 (56.1)	6.8 (6.9)	18.0 (17.8)		2.01	1.99
[Co(OBu^{t}N$_3$C$_6$H$_4$NO$_2$-4)$_2$]	21	44.9 (45.1)	4.8 (4.9)	21.3 (21.3)		2.01	2.08
[Co(OPr^{n}N$_3$C$_6$H$_4$Cl-4)$_2$]	6	44.9 (44.7)	4.3 (4.5)	17.5 (17.4)	12.2 (12.1)	2.11	2.12
[Co(OPr^{n}N$_3$C$_6$H$_4$Br-4)$_2$]	6	37.8 (37.7)	3.4 (3.8)	14.5 (14.7)	27.5 (27.9)	1.90	1.90
[Co(OPr^{n}N$_3$C$_6$H$_3$Me$_2$-2,3)$_2$]	5	56.7 (56.1)	6.5 (6.8)	17.5 (17.8)		1.90	1.95
[Co(OPr^{n}N$_3$C$_6$H$_3$Me$_2$-2,4)$_2$]	5	56.5 (56.1)	6.7 (6.8)	18.3 (17.8)		1.90	2.00
[Co(OPr^{n}N$_3$C$_6$H$_3$Me$_2$-2,6)$_2$]	5	56.1 (56.1)	6.9 (6.8)	18.0 (17.8)		1.95	2.02
[Co(OPr^{n}N$_3$C$_6$H$_3$Me-2-NO$_2$-4)$_2$]	10	45.2 (45.1)	4.9 (4.9)	21.2 (21.3)		2.18	2.03
[Co(OPr^{n}N$_3$Ph)$_2$]	5	52.1 (52.1)	5.7 (5.8)	20.0 (20.2)		2.04	1.99
[Co(OPr^{n}N$_3$C$_6$H$_4$Me-4)$_2$]	5	54.0 (54.2)	6.2 (6.3)	19.0 (19.0)		1.97	2.00
[Co(OPr^{n}N$_3$C$_6$H$_4$Me-2)$_2$]	5	54.3 (54.2)	6.3 (6.3)	18.9 (19.0)		2.00	1.93
[Co(OPhN$_3$Ph)$_2$]	10	57.9 (57.9)	4.3 (4.2)	17.3 (17.4)		1.91	2.04
[Co(OPhN$_3$C$_6$H$_4$Me-4)$_2$]	25	60.0 (60.1)	4.8 (4.7)	16.7 (16.4)		1.93	1.99
[Co(OPhN$_3$C$_6$H$_4$CO$_2$Et-4)$_2$]	50	57.4 (57.4)	4.6 (4.5)	13.6 (13.4)		4.49	4.57
[Co(OPhN$_3$C$_4$H$_4$Br-4)$_2$]	50	44.7 (44.9)	2.6 (2.8)	13.3 (13.2)		1.90	1.96

[a] Calculated values in parentheses. [b] Volume of MeOH used for dissolving 5 mmol of ligand. [c] Volume of water added to MeOH solution of ligand. [d] The complex was dried at 100 °C *in vacuo* to remove solvated water. [e] Synthesis carried out in MeNO$_2$; the complex recrystallised from boiling pyridine and dried at 100 °C *in vacuo*.

Table 2 Conditions of precipitation of cobalt(II) chelates from dmf, elemental analyses and magnetic data

	Mass of complex (mg)/dmf volume	Analysis (%)*				
Complex	(cm^3)	C	H	N	X	$\mu_{293 K}$
[Co(OMeN$_3$Ph)$_2$]	920/30	46.9 (46.8)	4.5 (4.5)	23.5 (23.4)	—	4.30
[Co(OMeN$_3$C$_6$H$_4$Me-4)$_2$]	810/50	49.6 (49.6)	5.0 (5.2)	21.7 (21.7)	—	2.08
[Co(OMeN$_3$C$_6$H$_4$Br-4)$_2$]	250/165	32.2 (32.5)	2.6 (2.7)	15.7 (16.2)	29.8 (30.9)	3.07
[Co(OMeN$_3$C$_6$H$_4$Cl-4)$_2$]	500/200	40.0 (39.3)	3.4 (3.3)	20.1 (19.6)	15.9 (16.6)	3.27

* Calculated values in parentheses.

Scheme 1
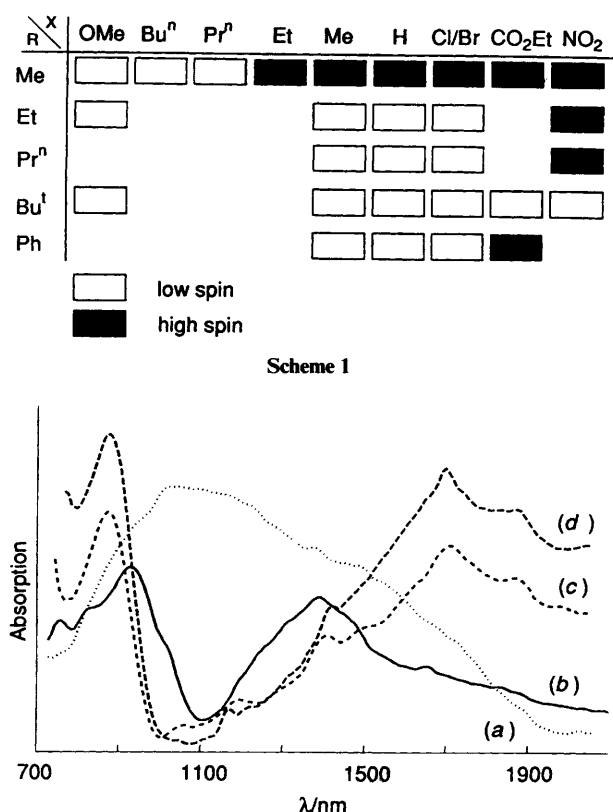
Fig. 1 Diffuse reflectance spectra of (a) high-spin [Co(OMeN$_3$-C$_6$H$_4$Me-4)$_2$], (b) [Co(OMeN$_3$C$_6$H$_4$NO$_2$-4)$_2$], (c) [Co(OEtN$_3$Ph)$_2$] and (d) [Co(OEtN$_3$C$_6$H$_3$Me$_2$-2,6)$_2$]

Fig. 2 The FIR spectra of (a) [Co(OEtN$_3$Ph)$_2$], (b) [Co(OMeN$_3$-C$_6$H$_4$OMe-4)$_2$], (c) high-spin [Co(OMeN$_3$C$_6$H$_4$Me-4)$_2$] and (d) high-spin [Co(OMeN$_3$Ph)$_2$]

absorption. The structure was solved and refined as above using SHELXS 90[12] and SHELX 76[13] programs. In the final cycle of calculations the H-atom positional and individual isotropic parameters were refined. Refinement converged at $R = 0.0271$, $R' = 0.0291$ [$w = 1/(\sigma_F^2 + 0.0018F^2)$]; final $(\Delta/\sigma)_{max} = 0.02$; $-0.42 < \Delta\rho < 0.24$ e Å^{-3} in final ΔF map. Scattering factors were those incorporated in the programs and from the literature.[14]

X-Ray powder diffractograms of [Ni(OMeN$_3$C$_6$H$_4$Me-4)$_2$] and low-spin [Co(OMeN$_3$C$_6$H$_4$Me-4)$_2$] were recorded on a Siemens type D 5000 diffractometer.

Additional material for both structures available from the Cambridge Crystallographic Data Centre comprises H-atom coordinates, thermal parameters and remaining bond lengths and angles.

Results and Discussion

Magnetic and Spectroscopic Characterisation of Low- and High-spin Bis(chelates).—From the magnetic data given in Table 1 it is seen that both high- and low-spin complexes might be isolated as the products of the standard synthesis in boiling methanol. The low-spin chelates show virtually constant magnetic moments of about 1.9–2.1 in the temperature range 77–300 K. The magnetic susceptibility measurements for [Co(OEtN$_3$Ph)$_2$] carried out down to 4.2 K did not reveal any anomalies at lower temperature. The high-spin chelates exhibit magnetic moments of 4.6–5.1, depending on the system, which are also virtually temperature independent between 77 and 300 K. Below 77 K the magnetic moments decrease smoothly reaching values of about 3.5 at 4.2 K.

Analysis of the magnetic data demonstrates the following dependencies between ligand substituents and the spin state of the bis(chelate): for ligands bearing a methyl group in one or both *ortho* positions of the phenyl ring the complexes thereof are without exception low spin; for ligands with unsubstituted
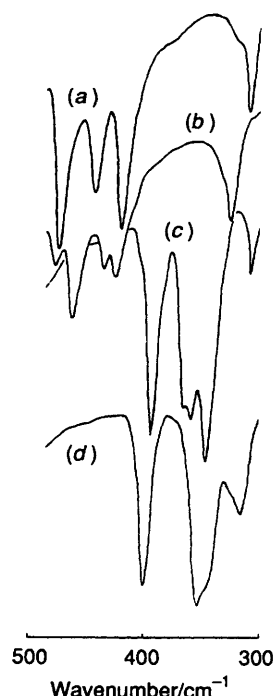
ortho positions both high- and low-spin bis(chelates) are possible depending on the substituent in the *para* position. For the sake of clarity, the situation for the latter class is depicted in Scheme 1. The *para* substituents are given in order of increasing polar effect,[15] the alkyl substituents in order of increasing size.

The complexes of 2-Me-6-XC$_6$H$_3$N$_3$ROH (X = Cl or Me) ligands were previously thoroughly characterised by means of magnetic and spectroscopic methods[16,17] and found to be low spin both in the solid state and solution. To date, no data on the cobalt(II) complexes of *ortho* unsubstituted triazene 1-oxides are available.

Typically the low-spin complexes are chocolate-brown to gold-brown whereas the high-spin complexes are bright red. The diffuse reflectance spectra of the low-spin chelates reveal a characteristic narrow band at about 11 500 cm^{-1} (870 nm) and a more intense shoulder at about 17 000 cm^{-1} (588 nm). This pattern is in line with the solution spectra of low-spin [Co(ORN$_3$C$_6$H$_3$Me-2-X-6)$_2$] (X = Me or Cl; μ = 2.1 in benzene solutions) described by Zacharias and Chakravorty.[16] The most characteristic feature of the corresponding spectra of the high-spin systems is the broad asymmetric band with the maximum at about 9000 cm^{-1} (1100 nm, see Fig. 1), most likely resulting from a superposition of two bands. For complexes with a nitro group in *para* position two bands are clearly seen at about 7250 and 11 000 cm^{-1} (1380 and 910 nm respectively).

The FIR spectra of the bis(chelates) are also diagnostic for the spin state, revealing strong bands in the ranges 300–400 and 400–500 cm^{-1} for high- and low-spin systems, respectively and related to the Co–O and Co–N stretching frequencies (see Fig. 2).

Molecular Structure of High- and Low-spin Complexes.—In a previous communication[2j] we reported the molecular structure of low-spin square-planar, centrosymmetric [Co(OEtN$_3$Ph)$_2$]. Here the structure of high-spin [Co(OMeN$_3$C$_6$H$_4$Me-4)$_2$] is presented. For the latter system the isolation of the low-spin isomer is also possible (see below). As we were not able to grow an X-ray-quality crystal of low-spin [Co(OMeN$_3$C$_6$H$_4$Me-4)$_2$] the molecular structure of the corresponding nickel(II) complex has been determined. X-Ray powder diffraction studies revealed

Table 3 Atomic coordinates for high-spin [Co(OMeN₃C₆H₄Me-4)₂]

Atom	x	y	z
Co	0.150 21(7)	0.005 68(5)	0.265 59(4)
O(1)	0.300 0(3)	−0.007 1(2)	0.376 7(2)
O(1')	−0.008 7(3)	−0.178 2(2)	0.229 6(2)
N(1)	0.265 7(4)	−0.100 4(3)	0.459 1(2)
N(2)	0.155 0(4)	−0.170 7(3)	0.458 9(2)
N(3)	0.079 0(4)	−0.141 3(3)	0.368 5(2)
N(1')	0.026 1(4)	0.191 1(3)	0.110 5(2)
N(2')	0.141 0(4)	0.099 5(3)	0.035 8(2)
N(3')	0.221 1(3)	−0.007 7(3)	0.090 1(2)
C(1)	−0.040 3(4)	−0.220 8(3)	0.364 0(3)
C(2)	−0.112 4(5)	−0.206 2(3)	0.266 1(3)
C(3)	−0.229 7(5)	−0.280 1(3)	0.254 8(3)
C(4)	−0.277 6(5)	−0.373 4(3)	0.339 9(3)
C(5)	−0.204 0(5)	−0.388 4(4)	0.437 3(3)
C(6)	−0.088 9(5)	−0.313 4(3)	0.451 0(3)
C(7)	−0.405 9(6)	−0.453 5(4)	0.329 2(3)
C(8)	0.360 5(5)	−0.120 5(4)	0.551 9(3)
C(1')	0.351 5(4)	−0.110 6(3)	0.010 6(3)
C(2')	0.428 5(5)	−0.231 9(3)	0.060 8(3)
C(3')	0.558 3(5)	−0.337 6(3)	−0.010 4(3)
C(4')	0.616 9(4)	−0.326 7(3)	−0.133 3(3)
C(5')	0.540 7(5)	−0.205 9(4)	−0.183 3(3)
C(6')	0.410 9(5)	−0.098 5(3)	−0.113 5(3)
C(7')	0.758 9(5)	−0.443 2(4)	−0.209 9(3)
C(8')	−0.079 3(5)	0.315 6(3)	0.068 1(3)

Table 4 Atomic coordinates for [Ni(OMeN₃C₆H₄Me-4)₂]

Atom	x	y	z
Ni	0.5000(—)	0.5000(—)	0.5000(—)
O(1)	0.2614(2)	0.5251(2)	0.5627(2)
N(1)	0.1748(2)	0.7158(2)	0.4845(2)
N(2)	0.2601(2)	0.8479(2)	0.3864(2)
N(3)	0.4314(2)	0.7725(2)	0.3711(2)
C(1)	0.5324(2)	0.9193(3)	0.2692(2)
C(2)	0.6587(3)	0.8809(3)	0.1595(3)
C(3)	0.7546(3)	1.0249(3)	0.0560(3)
C(4)	0.7288(3)	1.2057(3)	0.0613(3)
C(5)	0.6040(3)	1.2408(3)	0.1727(3)
C(6)	0.5051(3)	1.1002(3)	0.2762(3)
C(7)	0.8307(4)	1.3625(4)	−0.0572(5)
C(8)	−0.0159(3)	0.7600(3)	0.5205(3)
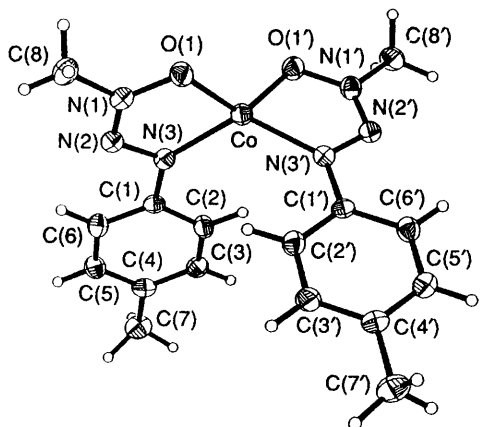
Fig. 3 An ORTEP diagram of high-spin [Co(OMeN₃C₆H₄Me-4)₂]

Table 5 Principal bond lengths and angles[a] for high-spin [Co-(OMeN₃C₆H₄Me-4)₂] **1**, [Ni(OMeN₃C₆H₄Me-4)₂] **2** and low-spin [Co(OEtN₃Ph)₂] **3**[b]

	1		**2**	**3**
	( )	(')		
M–O(1)	1.965(3)	1.964(2)	1.846(1)	1.813(3)
M–N(3)	1.981(3)	1.974(2)	1.876(2)	1.861(3)
O(1)–N(1)	1.346(3)	1.349(3)	1.356(2)	1.340(4)
N(1)–N(2)	1.281(4)	1.283(4)	1.279(2)	1.278(5)
N(1)–C(8)	1.457(5)	1.461(5)	1.456(3)	1.448(6)
N(2)–N(3)	1.335(4)	1.329(4)	1.327(2)	1.322(5)
N(3)–C(1)	1.420(5)	1.419(4)	1.434(2)	1.430(5)
O(1)–M–O(1')	123.5(1)			
O(1)–M–N(3)	79.8(1)		83.0(1)	82.4(1)
O(1)–M–N(3')	129.9(1)			
O(1')–M–N(3)	127.7(1)			
O(1')–M–N(3')	79.7(1)			
N(3)–M–N(3')	123.4(1)			
M–O(1)–N(1)	109.7(2)	109.2(2)	110.0(1)	111.4(2)
O(1)–N(1)–N(2)	123.0(3)	123.5(3)	120.5(1)	119.9(3)
O(1)–N(1)–C(8)	117.4(3)	116.4(3)	116.7(2)	118.2(3)
N(2)–N(1)–C(8)	119.6(3)	120.1(3)	122.8(2)	121.3(4)
N(1)–N(2)–N(3)	112.7(3)	111.8(3)	112.0(1)	110.9(3)
M–N(3)–N(2)	114.8(2)	115.6(2)	114.6(1)	115.3(2)
M–N(3)–C(1)	131.3(2)	130.7(2)	132.3(1)	133.3(3)
N(2)–N(3)–C(1)	113.8(2)	113.6(2)	112.9(1)	111.4(3)

[a] Valency angles listed only for symmetry-independent atoms. [b] Data from ref. 2(j).
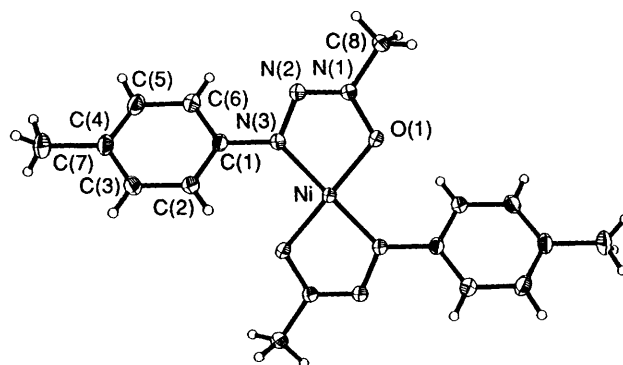
Fig. 4 An ORTEP diagram of [Ni(OMeN₃C₆H₄Me-4)₂]

the isomorphism of [Ni(OMeN₃C₆H₄Me-4)₂] and the low-spin isomer of [Co(OMeN₃C₆H₄Me-4)₂]. Atomic coordinates for the two complexes are given in Tables 3 and 4, respectively, ORTEP[18] drawings are depicted in Figs. 3 and 4, and principal bond lengths and angles together with those determined for [Co(OEtN₃Ph)₂] are collected in Table 5. It is to be noted that

all the bond lengths (apart from metal–ligand ones) and angles as well as the ligand conformation are virtually identical for low-spin [Co(OEtN₃Ph)₂] and centrosymmetric [Ni(OMe-N₃C₆H₄Me-4)₂]. The above evidence provides a sound indication that low-spin [Co(OMeN₃C₆H₄Me-4)₂] and [Ni-(OMeN₃C₆H₄Me-4)₂] are isomorphous and isostructural as well.

Whereas, similarly to all nickel(II) triazene 1-oxide complexes,[2a,l,r] [Ni(OMeN₃C₆H₄Me-4)₂] is square planar, high-spin [Co(OMeN₃C₆H₄Me-4)₂] reveals pseudo-tetrahedral coordination about the cobalt atom, with the chelate planes being perpendicular. Analysis of the data from Table 5 indicates that apart from the difference in bulk geometry the most conspicuous difference between high-spin [Co(OMeN₃C₆H₄-Me-4)₂] and [Co(OEtN₃Ph)₂] concerns the metal–ligand bond lengths. This is due to the change in spin state on going from a planar to a tetrahedral cobalt(II) complex. It is commonly accepted that a change in the occupancy of the antibonding d orbitals produces an appreciable alteration in the equilibrium metal–ligand bond distances.[19] For instance, the differences between average Fe–N bond lengths of high- and low-spin (ΔS = 2) isomers of [Fe(phen)₂(NCS)₂] (phen = 1,10-phenanthroline), [Fe(amp)₃]Cl₂·MeOH and [Fe(amp)₃]Cl₂·EtOH
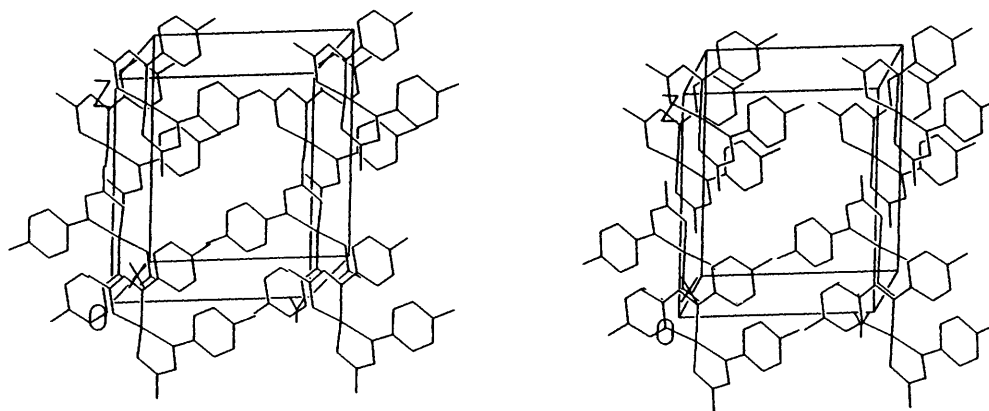
Fig. 5 Stereoview of the unit cell of high-spin [Co(OMeN$_3$C$_6$H$_4$Me-4)$_2$]. Molecules from neighbouring cells are included to show the stacking interactions. The hydrogen atoms have been removed for clarity
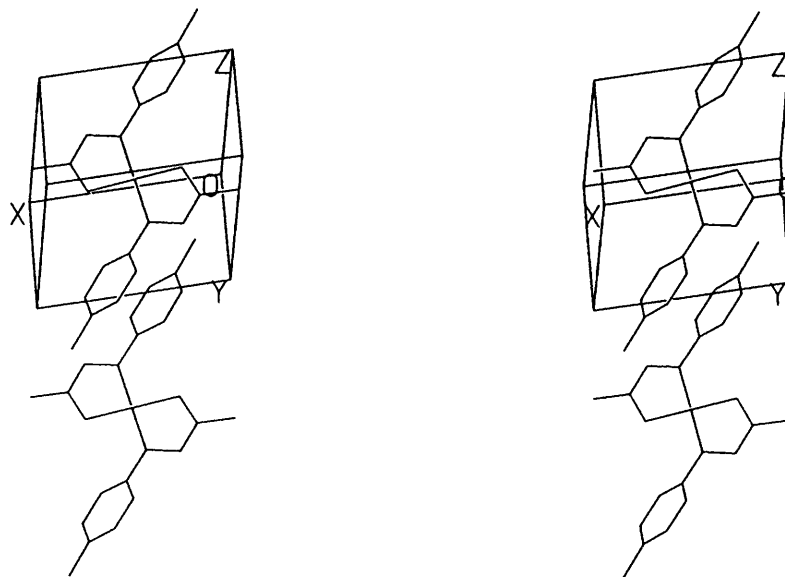

Fig. 6 Stereoview of the unit cell of high-spin [Ni(OMeN$_3$C$_6$H$_4$Me-4)$_2$]. Molecules from neighbouring cells are included to show the stacking interactions. The hydrogen atoms have been removed for clarity

(amp = 2-aminomethylpyridine) are 0.164,[20] 0.192[21a] and 0.182 Å.[21b] respectively. Shannon and Prewitt[22] estimated the differences in ionic radii for high- and low-spin ions to be 0.085 Å for Co^{II}. This value is in agreement with rather scarce experimental data: the average metal–ligand bond distance in low-spin [Co(salen)]·py[23] [H$_2$salen = N,N'-ethylenebis(sali-cylideneimine), py = pyridine] is 0.08 Å less than that in high-spin [Co(3MeO-salen)]·H$_2$O.[24] Extended X-ray absorption fine structure (EXAFS) measurements of the average metal–ligand bond length change, $\overline{\Delta R}$, for the spin crossover [Co(3CO$_2$H-salen)]·2$_2$OH and [Co(3CO$_2$H-salen)]·2py complexes yielded values of 0.08 and 0.12 Å, respectively.[25] For high-spin [Co(OMeN$_3$C$_6$H$_4$Me-4)$_2$] and [Co(OEtN$_3$Ph)$_2$] the differences between Co–O and Co–N(3) bond lengths are 0.15 and 0.12 Å, respectively. The difference in the metal–ligand bond strength is also reflected by the above-mentioned shift of the Co–N and Co–O stretching vibrations in the FIR region towards higher frequencies on going from high- to low-spin systems. No distinct differences in the remaining interatomic distances and angles are observed. Still, there is a substantial change in ligand conformation on going from the planar to the tetrahedral complex: the values of π, the interplanar angle between the chelate and aromatic ring planes, are 39.2° for low-spin [Co(OEtN$_3$Ph)$_2$], 39.4° for [Ni(OMeN$_3$C$_6$H$_4$Me-4)$_2$], 5.3 and 6.8° for the non-equivalent ligands in high-spin [Co(OMeN$_3$C$_6$H$_4$Me-4)$_2$].

The crystal lattice of high-spin [Co(OMeN$_3$C$_6$H$_4$Me-4)$_2$]

contains intermolecular stacking interactions of two distinct types, i.e. stacking between planar NNNO fragments and stacking between NNNO and phenyl ring moieties. For each molecule with a cobalt atom placed at x, y, z the N(1)–N(2)–N(3)–O(1) fragment is parallel to the N(1)–N(2)–N(3)–O(1) fragment of the molecule with the cobalt atom placed at $-x$, $-y$, 1 − z (stacking A). The distance between the planes is 3.37(2) Å, the shortest contact being that between the N(1) and N(3) atoms (3.38 Å). On the other hand, the second ligand is positioned in a head-to-tail manner as regards the neighbouring ligand of a third molecule with a cobalt atom placed at 1 − x, −y, −z. The angle between the normals to the interacting N(1')–N(2')–N(3')–O' and C(1')–C(6') planes is in this case 172°, the shortest contact being that between N(3') and C(6') (3.47 Å, stacking B). It is important to note that in both cases the cobalt atoms are not involved in any interaction, the effective co-ordination number being four. The phenyl rings of the ligands involved in stacking A do not undergo any specific interactions.

Only one type of stacking interactions has been found in the planar [Ni(OMeN$_3$C$_6$H$_4$Me-4)$_2$] chelate, i.e. between the phenyl rings of adjacent molecules. The phenyl rings are parallel, the distance between their planes being 3.28(2) Å, and the shortest distance is that between the C(2) and C(3) atoms (3.32 Å). The intermolecular stackings discussed above are depicted in Figs. 5 and 6. It is noteworthy that for two high-spin triazene 1-oxide bis(chelates) characterised previously by X-ray
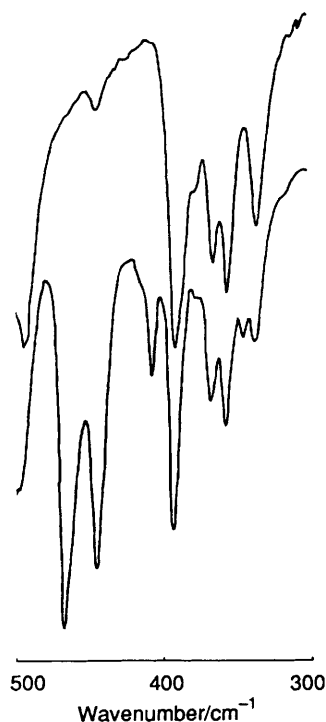
Fig. 7 The FIR spectra of $[Co(OMeN_3C_6H_4Cl-4)_2]$ synthesised by the standard method (top) and precipitated from dmf (bottom)

methods, *i.e.* $[Co(OEtN_3C_6H_4OMe-2)_2]^{2n}$ and $[Co(OMeN_3-C_6H_4Cl-2)_2],^{2q}$ a tetrahedral or slightly flattened tetrahedral geometry of the CoN_2O_2 core has been found. Nevertheless, in those chelates, additional interactions involving the cobalt and chlorine or methoxy oxygen atoms are crucial for achieving the high-spin configurations.

The Isolation of Spin Isomers.—The strong dependence of the spin state upon ligand substituents for systems synthesised according to the standard method, as well as the previously reported observations of high spin–low spin conversions,[2j] prompted us to demonstrate the possibility of isolating the low-spin isomers of those bis(chelates) which are generally obtained in the high-spin form. We found that dissolving some of the high-spin complexes in dmf followed by precipitation with water yielded samples showing the presence of low-spin complexes, as indicated by ESR data.[2j] Therefore a study of complexes precipitated from dmf was carried out for $[Co(OMeN_3Ph)_2],[Co(OMeN_3C_6H_4Me-4)_2],[Co(OMeN_3C_6-H_4Cl-4)_2]$ and $[Co(OMeN_3C_6H_4Br-4)_2]$, which are high spin if prepared according to the standard method (*i.e.* synthesis in boiling MeOH).

The details of those experiments are given in the Experimental section. The elemental analysis data and the IR spectra show that no water or dmf molecules are present in the samples obtained (see Table 2). In the case of $[Co(OMeN_3C_6H_4Me-4)_2]$ the procedure resulted in the complete conversion of the high-into the low-spin isomer, the magnetic moment of which is 2.08 at room temperature (r.t.). The diffuse reflectance spectrum reveals the presence of a narrow band at 11 700 cm^{-1} and a shoulder at about 16 700 cm^{-1}, providing incontrovertible evidence for the presence of a low-spin, planar, four-co-ordinate bis(chelate). Also the FIR spectrum, exhibiting three strong bands between 400 and 500 cm^{-1}, fits the pattern found for the planar low-spin complexes. The isolated low-spin isomer is isomorphous with the centrosymmetric $[Ni(OMeN_3C_6H_4-Me-4)_2]$, the structure of which was given above.

In the case of $[Co(OMeN_3C_6H_4Cl-4)_2]$ and $[Co-(OMeN_3C_6H_4Br-4)_2]$ the magnetic moments for the complexes were 3.27 and 3.07, respectively, indicating that about 30% of the
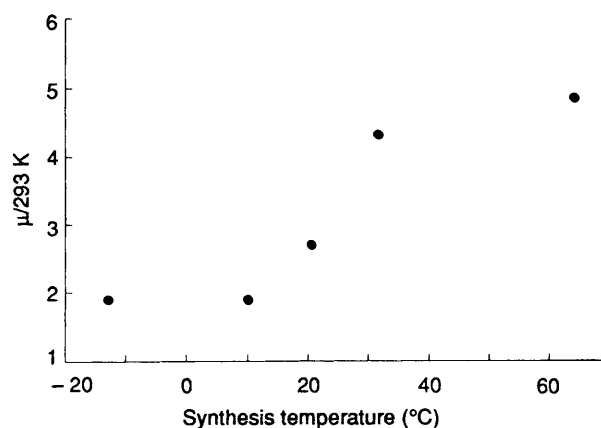
Fig. 8 Dependence of the magnetic moment of $[Co(OMeN_3C_6H_4-Me-4)_2]$ on synthesis temperature

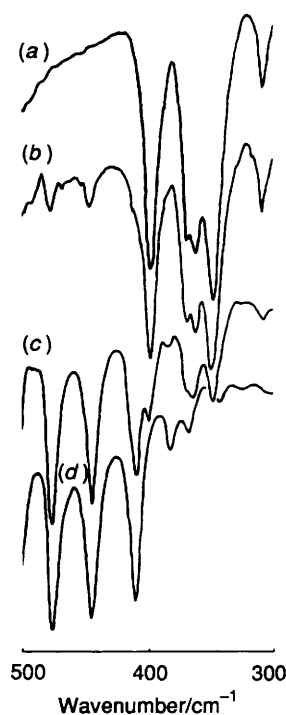**Fig. 9** The FIR spectra of $[Co(OMeN_3C_6H_4Me-4)_2]$ synthesised in MeOH at (*a*) 64.7, (*b*) 31.5, (*c*) 21.5 and (*d*) 10 °C

high-spin isomer is still present. This finds support in FIR spectra, in which bands corresponding to the high- and low-spin isomers are seen (see Fig. 7). On the other hand, for $[Co(OMeN_3Ph)_2]$ only a slight decrease of the magnetic moment was found (4.3) implying that a rather limited conversion took place.

Attempts to dissolve the mixtures of spin isomers of $[Co(OMeN_3C_6H_4Br-4)_2]$ and $[Co(OMeN_3C_6H_4Cl-4)_2]$ in toluene resulted in their conversion into the bright red high-spin tetrahedral isomers which were deposited after few minutes. The same effect has been observed for pure low-spin $[Co(OMeN_3C_6H_4Me-4)_2]$. For the latter the precipitation of the high-spin isomer occurs much more slowly and one can initially obtain a transparent solution.

The second part of the experiments concerned the influence of the temperature of preparation in methanol upon the spin states of the solid complexes formed. A series of syntheses of $[Co(OMeN_3C_6H_4Me-4)_2]$ and other complexes in methanol at different temperatures were carried out. The most striking results were obtained in the case of $[Co(OMeN_3C_6H_4Me-4)_2]$ and $[Co(OMeN_3C_6H_4Et-4)_2]$. In the latter case the synthesis in boiling methanol yielded the pure high-spin isomer with a magnetic moment of 4.78 (r.t.). The synthesis carried out at

Table 6 Fraction of high-spin isomer for [Co(OMeN$_3$C$_6$H$_4$Me-4)$_2$] synthesised at different temperatures

T/°C	μ$_{293}$	x_{hs} From magnetism	From FIR
−13	1.90	0.0	0.0
10	1.90	0.0	0.0
20.5	2.70	0.185	0.185
31.5	4.32	0.756	0.850*
64	4.85	1.0	1.0

* Poorly developed low-spin isomer bands.

Fig. 10 Electronic spectra of [Co(OMeN$_3$C$_6$H$_3$Me$_2$-2,6)$_2$] (———), [Co(OMeN$_3$C$_6$H$_4$Me-2)$_2$] (— — — —), [Co(OPr^{n}N$_3$C$_6$H$_3$Me-2-NO$_2$-4)$_2$] (— · —), [Co(OMeN$_3$C$_6$H$_4$CO$_2$Et-4)$_2$] (– – –), [Co(OEtN$_3$Ph)$_2$] (– – –) and [Co(OMeN$_3$Ph)$_2$] (· · · · ·). Solvent: CH$_2$Cl$_2$. Concentrations are 0.05 mol dm^{-3}

−15 °C resulted in the formation of the low-spin isomer, its IR and diffuse reflectance spectra being typical for four-co-ordinate square-planar complexes. For [Co(OMeN$_3$C$_6$H$_4$Me-4)$_2$] the syntheses were carried out at several temperatures, *i.e.* −13, 10, 20.5 and 31.5 °C and in boiling methanol. The dependence of the magnetic moment on the synthesis temperature is illustrated in Fig. 8. Upon increasing the temperature of synthesis an increase in magnetic moment was observed. The FIR spectra reveal that in syntheses at 20.5 and 31.5 °C a conglomerate of square-planar and tetrahedral isomers was obtained (see Fig. 9).

An attempt to determine the mole fractions of the high-spin isomer has been undertaken on the basis of the magnetic and FIR data. Assuming the magnetic moments of the two isomers to be 4.85 and 1.90, the mole fraction of high-spin molecules was calculated on the basis of the known Wiedemann formula (1)

$$\mu^2 = \mu_1^2 x_1 + \mu_2^2(1 - x_1) \qquad (1)$$

where μ = magnetic moment of resulting conglomerate of isomers, μ$_1$ = magnetic moment of pure high-spin isomer, μ$_2$ = that of low-spin isomer and x$_1$ = mole fraction of high-spin isomer. The FIR spectra of a series of mixtures prepared from pure high- and low-spin isomers of [Co(OMeN$_3$C$_6$H$_4$-Me-4)$_2$] were recorded. From measurements of the relative intensities of the bands characteristic for the planar and tetrahedral isomers a standard plot of the relative intensities *vs.* high-spin mole fraction was determined. The mole fraction of the high-spin isomer in samples prepared at different temperatures was then estimated using this plot. The results are given in Table 6.

The FIR spectra of low-spin [Co(OMeN$_3$C$_6$H$_4$Me-4)$_2$] synthesised in MeOH at 10 °C are identical with those of the low-spin isomer precipitated from dmf.

Whereas for [Co(OMeN$_3$C$_6$H$_4$Me-4)$_2$] and [Co(OMeN$_3$-C$_6$H$_4$Et-4)$_2$] we succeeded in the isolation of both spin isomers, in the case of ligands with longer alkyl chains occupying the *para* position of the aromatic ring, *i.e.* for [Co(OMeN$_3$C$_6$H$_4$-Pr^n-4)$_2$] and [Co(OMeN$_3$C$_6$H$_4$Bu^n-4)$_2$], only the low-spin complexes were obtained even if the syntheses were carried out in boiling methanol. On the other hand [Co(OMeN$_3$C$_6$H$_4$-Me-3)$_2$] and [Co(OMeN$_3$Ph)$_2$] do not give any noticeable amounts of low-spin isomers even if synthesised at −15 °C (in the latter case water should be added to precipitate the complex), similarly to [Co(OMeN$_3$C$_6$H$_4$Cl-4)$_2$] and [Co-(OMeN$_3$C$_6$H$_4$Br-4)$_2$]. Therefore the syntheses of the above complexes were carried out at about −60 °C, using a Pr^{i}OH–solid CO$_2$ cooling bath. A pure low-spin isomer was obtained (μ = 1.90, 295 K) only for [Co(OMeN$_3$C$_6$H$_4$Me-3)$_2$]; [Co-(OMeN$_3$Ph)$_2$] and [Co(OMeN$_3$C$_6$H$_4$Cl-4)$_2$] exhibit magnetic moments of 3.98 and 3.78 at 295 K, respectively, indicating that about 60% of the high-spin isomer is present in the conglomerates.

No attempts at low-temperature syntheses were made for [Co(OMeN$_3$C$_6$H$_4$CO$_2$Et-4)$_2$] and complexes of nitro-substituted ligands. For the former the aqua-adduct was isolated even if synthesised at 20 °C (the tetrahedral complex
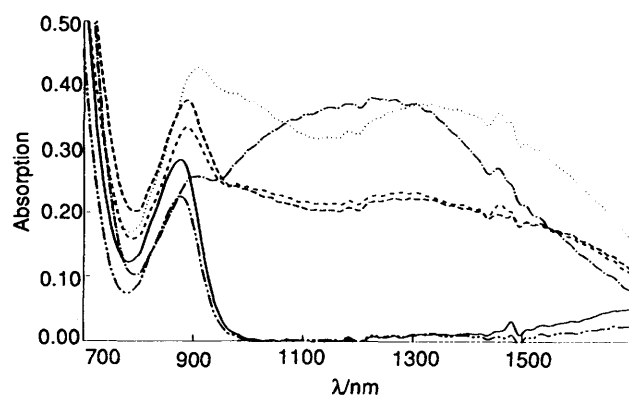
was obtained by drying the adduct at 100 °C *in vacuo*), whereas the low solubility of nitro-substituted ligands precluded the isolation of pure chelates at −60 °C. For the latter the synthesis or recrystallisation from dmf yielded the dmf adducts. It should be emphasised that the influence of the synthesis temperature on the composition of spin-isomer conglomerates does not seem to be related to a possible planar–tetrahedral equilibrium in methanol. Such equilibria were established for solutions in non-co-ordinating solvents (see below), however in methanol the results of NMR and ESR measurements indicate the presence of high-spin species only. The thermogravimetric curves of low-spin complexes do not reveal the presence of any endothermic processes at temperatures below the melting points. Melting of the studied complexes results in their subsequent decomposition. We have found, however, that heating of low-spin [Co(OMeN$_3$C$_6$H$_4$Me-4)$_2$] at 118 °C *in vacuo* (drying pistol, butanol) over 150 h produces a gradual conversion into the high-spin isomer, yielding eventually about 20% of the latter as detected by FIR spectra. The gradual nature of this process suggests that the spin conversion in solid state does not have the character of a phase transition and therefore is most likely facilitated by lattice defects.

The syntheses of low- and high-spin isomers of triazene 1-oxide cobalt(II) chelates provide the first case of the isolation of planar and tetrahedral isomers of four-co-ordinate cobalt(II) complexes. Known cobalt(II) bis(chelates), exhibiting planar–tetrahedral equilibria in CHCl$_3$ solutions, *i.e.* N-substituted β-iminoamines and monothiodipivaloylmethanes are purely high- or low-spin in the solid state, although their magnetic moments in solution vary from 2.70 to 4.50 (r.t.).[4] Also for nickel(II) bis(chelates), for which square planar–tetrahedral equilibria are quite common in solution,[3] there have been no reports on such an isolation. Recently for some nickel(II) chelates [Ni{(O)PR$_2$NR'}$_2$] (R, R' = alkyl) the conglomerate crystallisation of spin isomers has been found.[3b-e]

The existence of both square-planar and distorted-tetrahedral isomers is a well recognised feature in the co-ordination chemistry of copper(II).[26] However, in these cases, isomerisation does not produce a change in spin multiplicities and there are no well defined energy minima corresponding to the planar and tetrahedral isomers.[3a] Still, there is a clear resemblance between some aspects of the distortion isomerism of copper(II) complexes and spin isomerism of cobalt(II) triazene 1-oxide bis(chelate) complexes, *i.e.* in the sensitivity of their structure to synthesis conditions such as temperature, solvent used, total solute concentration, *etc.*[26] For instance, apart from the effect of synthesis temperature, our preliminary data show that although it is rather difficult to achieve a high fraction of low-spin [Co(OMeN$_3$Ph)$_2$] from the synthesis carried out in MeOH, recrystallisation from cold acetone or very slow crystallisation

Table 7 Thermodynamic parameters of low spin $\rightleftharpoons$ high spin equilibria for cobalt(II) bis(chelates)[a]

Complex	Solvent	ΔH°/ kJ mol⁻¹	ΔS°/ J K⁻¹ mol⁻¹	x_{hs}^{293}
[Co(OEtN₃C₆H₃Me₂-2,6)₂][b,c]	C₆D₅CD₃			0.00
[Co(OBu^tN₃C₆H₄Me-4)₂][c]	CDCl₃			0.00
[Co(OMeN₃C₆H₄OMe-4)₂][c]	CDCl₃			0.02
[Co(OMeN₃C₆H₄Me-2)₂][b,c]	C₆D₅CD₃	15 ± 2	29 ± 5	0.07
[Co(OMeN₃C₆H₃Me₂-2,6)₂][b,c]	C₆D₅CD₃	14 ± 2	24 ± 5	0.07
[Co(OMeN₃Ph)₂][d]	CDCl₃	8 ± 2	20 ± 5	0.31
	C₆D₅CD₃	9 ± 2	24 ± 5	0.28
[Co(OEtN₃Ph)₂][c]	CDCl₃	7 ± 2	24 ± 5	0.46
	C₆D₅CD₃	11 ± 2	30 ± 5	0.29
[Co(OMeN₃C₆H₄Me-4)₂][d]	CDCl₃	10 ± 2	29 ± 5	0.32
[Co(OEtN₃C₆H₄Me-4)₂][c]	CDCl₃	9 ± 2	24 ± 5	0.33
[Co(OMeN₃C₆H₄Bu^n-4)₂][c]	CDCl₃	5 ± 2	12 ± 5	0.35
[Co(OEtN₃C₆H₄Cl-4)₂][c]	CDCl₃	6 ± 2	17 ± 2	0.36
[Co(OBu^tN₃C₆H₄NO₂-4)₂][c]	CDCl₃	3 ± 2	6 ± 5	0.35
[Co(OMeN₃C₆H₄CO₂Et-4)₂][d]	CDCl₃	1 ± 3	5 ± 5	0.53

[a] If not indicated otherwise, ΔH° and ΔS° were determined from data taken in the temperature range 214–313 K for CDCl₃ and 193–363 for C₆D₅CD₃ solutions. [b] Temperature range 296–368 K; x_{hs} given is that at 296 K. [c] Low spin in solid state. [d] High spin in solid state.
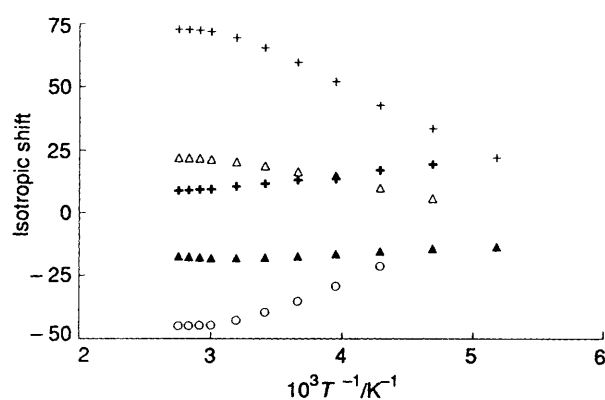

Fig. 11 Temperature dependence of isotropic shifts for [Co(OEtN₃Ph)₂] in C₆D₅CD₃: +, CH₃; △, CH₂; ○, o-H; +, m-H; ▲, p-H

from diluted methanolic solutions can lead to small amounts of almost pure low-spin isomer.

Planar–Tetrahedral Equilibria in Solutions of Non-co-ordinating Solvents.—The electronic spectra of some bis(chelates) are shown in Fig. 10. It is seen that for [Co(OMeN₃C₆H₄Me-2)₂] and [Co(OMeN₃C₆H₃Me₂-2,6)₂] only the band at $\approx 11\,700$ cm⁻¹ (855 nm) observed also for solid low-spin complexes is present. For the remaining complexes an additional band is observed at lower frequencies. As this band may be identified with that observed for solid high-spin complexes the simultaneous presence of planar (low-spin) and tetrahedral (high-spin) bis(chelates) is inferred. Virtually the same situation is observed in toluene solutions.

The NMR studies of a series of [Co(ORN₃C₆H₄X)₂] and [Co(ORN₃C₆H₃X₂)₂] chelates have shown a non-Curie dependence of the observed isotropic shifts, as exemplified in Fig. 11, indicating the possibility of spin-state equilibria. For solutions of complexes revealing the presence of bands due to both spin isomers, temperature-dependent magnetic susceptibility measurements have been carried out. From the latter temperature dependence the thermodynamic parameters of the low spin–high spin isomerisation have been elucidated assuming magnetic moments of 1.90 and 4.85 for low- and high-spin complexes, respectively. The results of these studies are collected in Table 7. Generally, in solutions of non-co-ordinating solvents, the complexes studied show a slight preference for the low-spin form independent whether the parent chelates are low- or high-spin in the solid state. On the whole, the magnetic moment increases with increasing tem-

perature. In one case, i.e. [Co(OMeN₃C₆H₄CO₂Et-4)₂], the magnetic moment is practically independent of temperature varying from 3.60 at 214.2 to 3.73 at 313.2 K. The values of ΔH° and ΔS° determined lie in the range observed previously for bis(β-iminoamine) complexes of cobalt(II) ($\Delta H^\circ = 0$–12 kJ mol⁻¹, $\Delta S^\circ = 6$–32 J K⁻¹ mol⁻¹).[3,4] The ΔS° values contain three principal contributions[27] [equation (2)] where ΔS_{el}°

$$\Delta S_{ls/hs}^\circ = \Delta S_{el}^\circ + \Delta S_{solv}^\circ + \Delta S_{vib}^\circ \qquad (2)$$

denotes the entropy change arising from an increase in the spin multiplicity (on going from a doublet to a quartet state, $\Delta S_{el}^\circ = R \ln 2 = 5.8$ J K⁻¹ mol⁻¹), ΔS_{solv}° is the entropy change due to the differing degrees of solvation of the planar and tetrahedral isomers, and ΔS_{vib}° represents the change in vibrational entropy. Assuming the last term to be of minor importance in our case, in the absence of bulky substituents on the N¹ atom and phenyl rings, ΔS° values of about 20–30 J K⁻¹ mol⁻¹ are observed suggesting that the planar form is the more highly and regularly solvated. A similar effect was observed for nickel(II) aminotropone iminate complexes (tropone = cyclohepta-2,4,6-trien-1-one).[3a] If more bulky substituents are present the ΔS° value decreases {cf. ΔS° for [Co(OMeN₃C₆H₄Bu^n-4)₂], [Co(OBu^tN₃C₆H₄NO₂-4)₂] and [Co(OMeN₃C₆H₄CO₂Et-4)₂]}.

The ΔH° values are without exception endothermic and reflect primarily the weakening of metal–ligand bond strengths on going from the low- to high-spin configuration.

Factors Determining the Structure of Triazene 1-Oxide Cobalt(II) Bis(chelates).—The main requirement for a bis(chelate) system to exhibit a planar–tetrahedral spin isomerism is that the ligand-field strength becomes close to the cross-over point. Indeed, the enthalpy changes determined for our systems are very small and comparable to those found for rotamers of simple organic molecules.[28] Therefore a subtle change in ligand substituents may produce a dramatic change in the structure of a given complex. Particularly, the isolation of both spin isomers becomes possible. Below we discuss some trends governing the geometry (and hence the spin state) of these bis(chelates).

(a) *Complexes bearing methyl groups in* ortho *positions of the ligand phenyl ring.* As can be seen from the data in Table 1 all complexes with methyl substituents in one or both ortho positions of the aromatic ring, i.e. bis(chelates) of [Co(ORN₃C₆H₃Me-2-X-4)₂] (X = H, Me or NO₂) and [Co(ORN₃C₆H₃Me₂-2,6)₂] type, are invariably low spin in the solid state. The steric clashes between the o-methyl group and the N² atom or the corresponding interactions between the methyl group and

Table 8 Cyclic voltammetry data for the cobalt(II) complexes[a]

Complex	$E_{298}^{\ominus(1)}/V$	$E_{298}^{\ominus(2)}/V$
$[Co(OMeN_3C_6H_3Me_2\text{-}2,6)_2]$	0.09	0.40[b]
$[Co(OEtN_3C_6H_3Me_2\text{-}2,6)_2]$	0.12	—
$[Co(OPrN_3C_6H_3Me_2\text{-}2,6)_2]$	0.13	—
$[Co(OBu^tN_3C_6H_3Me_2\text{-}2,6)_2]$	0.06	—
$[Co(OMeN_3C_6H_4Me\text{-}2)_2]$	0.13	0.46
$[Co(OEtN_3C_6H_4Me\text{-}2)_2]$	0.11	0.43
$[Co(OBu^tN_3C_6H_4Me\text{-}2)_2]$	0.06	—
$[Co(OMeN_3Ph)_2]$	0.12	0.48
$[Co(OEtN_3Ph)_2]$	0.09	0.41
$[Co(OMeN_3C_6H_4Me\text{-}4)_2]$	0.09	0.38
$[Co(OEtN_3C_6H_4Me\text{-}4)_2]$	0.06	0.33
$[Co(OBu^tN_3C_6H_4Me\text{-}4)_2]$	0.03	0.25[b]
$[Co(OMeN_3C_6H_4Et\text{-}4)_2]$	0.09	0.39
$[Co(OMeN_3C_6H_4CO_2Et\text{-}4)_2]$	0.21	0.69
$[Co(OMeN_3C_6H_4Me\text{-}3)_2]$	0.10	0.42
$[Co(OMeN_3C_6H_4OMe\text{-}4)_2]$	0.06	0.33
$[Co(OBu^tN_3C_6H_4CO_2Et\text{-}4)_2]$	0.18	0.59
$[Co(OMeN_3C_6H_4Cl\text{-}4)_2]$	0.13	0.72

[a] Platinum electrode; supporting electrolyte 0.1 mol dm^{-3} NBu$_4$ClO$_4$; CH$_2$Cl$_2$; all potentials are referenced to ferrocene–ferrocenium. [b] Small peaks with $I_{pa}^{(2)}/I_{pa}^{(1)} \leqslant 0.1$.

cobalt(II) atom, hindering a coplanar ligand conformation, seem likely to be the key factor. We have previously demonstrated that o-Me substitution of the ligand phenyl ring results in an increased ability for dioxygen binding upon co-ordination of a Lewis base to the bis(chelate), as compared with the adducts of complexes derived from $ortho$-unsubstituted ligands. Our incomplete neglect of differential overlap (INDO) calculations of the charge distribution in ligand anions demonstrated its dependence on ligand conformation. With increasing tilt of the aromatic ring towards the NNNO plane the amount of negative charge on the NNNO fragment increases, due to impaired conjugation between the phenyl ring and triazene 1-oxide linkage.[2k] The increase in charge on the latter might be roughly identified with an increase in the ligand's donor strength. Our preliminary MNDO calculations have shown that the proximity of an o-Me group and N^2 atom for a coplanar conformation of the free ligand gives rise to a rotation barrier of about 25 kJ mol^{-1}.[29] Thus the presence of o-Me substituents favours a non-coplanar conformation of ligand anions and hence results in an increased donor strength thereof. In fact, $\Delta H_{\text{ls/hs}}^{\ominus}$ for [Co(OMeN$_3$C$_6$H$_4$Me-2)$_2$] in CDCl$_3$ is significantly larger than those determined for complexes of $ortho$-unsubstituted ligands, the former displaying a strong stabilisation of the planar form. For ligands with an unsubstituted $ortho$ position the rotation about the N^3–C^1 bond is practically free,[29] facilitating tuning of the ligand donor properties to the stereoelectronic demands of the complex via alteration of the ligand conformation. Furthermore, for solid complexes the stacking interactions described for high-spin [Co(OMeN$_3$-C$_6$H$_4$Me-4)$_2$] should be hindered by a non-coplanar ligand conformation. Indeed, as mentioned above, there is an appreciable difference in conformation of the ligand in high-spin [Co(OMeN$_3$C$_6$H$_4$Me-4)$_2$] for which the ligand is almost exactly coplanar (π = 5.3, 6.8°), and that observed for low-spin [Co(OEtN$_3$Ph)$_2$] (π = 39.2°)[2j] or [Co(OMeN$_3$C$_6$H$_4$Me-4)$_2$] (π = 39.4°, isostructural with its nickel analogue). The values of π for [Ni(OMeN$_3$C$_6$H$_3$Cl-2-Me-6)$_2$] are 71 and 81° for the two non-equivalent ligands.[2c]

(b) *Complexes with ligands possessing a phenyl ring with an unsubstituted ortho position.*—For this class of bis(chelates) both planar and tetrahedral species may be obtained as the result of the standard synthesis in boiling methanol. For some complexes with R = Me, *i.e.* [Co(OMeN$_3$C$_6$H$_4$Me-4)$_2$], [Co(OMeN$_3$Ph)$_2$], [Co(OMeN$_3$C$_6$H$_4$Me-3)$_2$], [Co(OMeN$_3$-C$_6$H$_4$Cl-4)$_2$], [Co(OMeN$_3$C$_6$H$_4$Br-4)$_2$] and [Co(OMeN$_3$-

C$_6$H$_4$Et-4)$_2$], the isolation of both spin isomers or at least of their conglomerates is possible. An analysis of the data from Scheme 1 indicates some trends governing the formation of planar or tetrahedral complexes in the solid state. First, in the main the electron-withdrawing substituents in *para* position, such as nitro or ethoxycarbonyl, result in formation of high-spin complexes. This effect is quite obviously due to the weakening of the donor properties of the ligand as seen from our INDO calculations for the OMeN$_3$C$_6$H$_4$NO$_2$-4$^-$ anion.[2k] For complexes of such ligands {*i.e.* [Co(OMeN$_3$C$_6$H$_4$CO$_2$Et-4)$_2$] and [Co(OBu^{t}N$_3$C$_6$H$_4$NO$_2$-4)$_2$]} planar–tetrahedral equilibria are observed in solution, nevertheless the $\Delta H_{\text{ls/hs}}^{\ominus}$ values are significantly smaller than those determined for the remaining systems (*cf.* Table 7). On the other hand a pronounced stabilisation of the low-spin isomer has been found for [Co(OMeN$_3$C$_6$H$_4$OMe-4)$_2$] in CDCl$_3$.

The size of R and 4-X alkyl substituents seems to be the second important factor influencing the structure of the solid complexes. With increasing size of R the effect of an electron-withdrawing 4-X substituent is counterbalanced: for R = Me a number of high-spin complexes was isolated. For R = Et only [Co(OEtC$_6$H$_4$NO$_2$-4)$_2$] is high spin whereas for R = Bu^t all complexes are low spin. The above trend seems to be related primarily to packing effects.

Electrochemical Properties.—The redox activity of the complexes was studied in all cases by cyclic voltammetry (CV) in the potential range −1.8 to +1.0 V *versus* the ferrocene–ferrocenium redox system in dichloromethane solutions (0.1 mol dm^{-3} NBu$_4$ClO$_4$, 298 K). The formal potentials $E_{298}^{\ominus}$, calculated as the average of the cathodic (E_{pc}) and anodic (E_{pa}) peak positions, are given in Table 8, typical CV curves are depicted in Fig. 12.

No peaks corresponding to reduction have been observed down to −1.8 V. As the ligands were shown to be electrochemically inactive in the studied potential range the observed redox processes have been assumed to be metal-centred. For the studied cobalt(II) bis(chelates) one or two quasi-reversible, one-electron oxidations at $E_{298}^{\ominus(1)}$ = 0.03–0.12 V and $E_{298}^{\ominus(2)}$ = 0.25–0.72 V (ΔE_p = 100–120 mV, halfwidth = 70–80 mV) have been observed depending on the ligand structure. These potentials are significantly lower than those observed for high-spin pseudo-octahedral [Co(OMeN$_3$C$_6$H$_4$Cl-2)$_2$] and [Co(OMeN$_3$-C$_6$H$_4$OMe-2)$_2$].[2n] The potentials of both show a Hammett-type dependence on ligand substituents, increasing linearly with decreasing electron-releasing effect. The $E_{298}^{\ominus(2)}$ potentials are more susceptible to the polar effect [see (Fig. 13)].

All complexes display a cyclic response with characteristic anodic and cathodic peak potentials in the range 0.03–0.21 V due to the Co^{II} $\longrightarrow$ Co^{III} oxidation [equation (3)]. Single oxid-

$$[Co^{II}L_2] \rightleftharpoons [Co^{III}L_2]^+ + e^- \qquad (3)$$
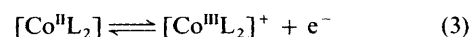
ations at $E_{298}^{\ominus(1)}$ were observed only for [CoL$_2$] chelates derived from o-Me (R = Bu^t) and 2,6-Me$_2$ (R = Et, Pr^n or Bu^t) substituted ligands. For the remaining chelates studied a second strong peak ($I_{pa}^{(2)}/I_{pa}^{(1)}$ = 0.3–0.53) corresponding to a successive one-electron oxidation at $E_{298}^{\ominus(2)}$ = 0.25–0.75 V has been observed. In two cases, [Co(OMeN$_3$C$_6$H$_3$Me$_2$-2,6)$_2$] and [Co(OBu^{t}N$_3$C$_6$H$_4$Me-4)$_2$], a relatively small CV response ($I_{pa}^{(2)}/I_{pa}^{(1)}$ = 0.1 and 0.07 respectively) was observed in the $E_{298}^{\ominus(2)}$ potential range. The origin of the second peak is not immediately obvious. Clearly, there is no correlation between the occurrence of the high-potential oxidation process, its peak height and the existence of high spin–low spin equilibria {see Tables 7 and 8, *cf.* [Co(OEtN$_3$C$_6$H$_3$Me$_2$-2,6)$_2$], [Co(OBu^t-N$_3$C$_6$H$_4$Me-4)$_2$] and [Co(OMeN$_3$C$_6$H$_4$OMe-4)$_2$]}. This is not unexpected as the high spin–low spin interconversion rate is much too large to allow the observation of individual spin isomers at the applied scan rates of 25–3200 mV s^{-1}.

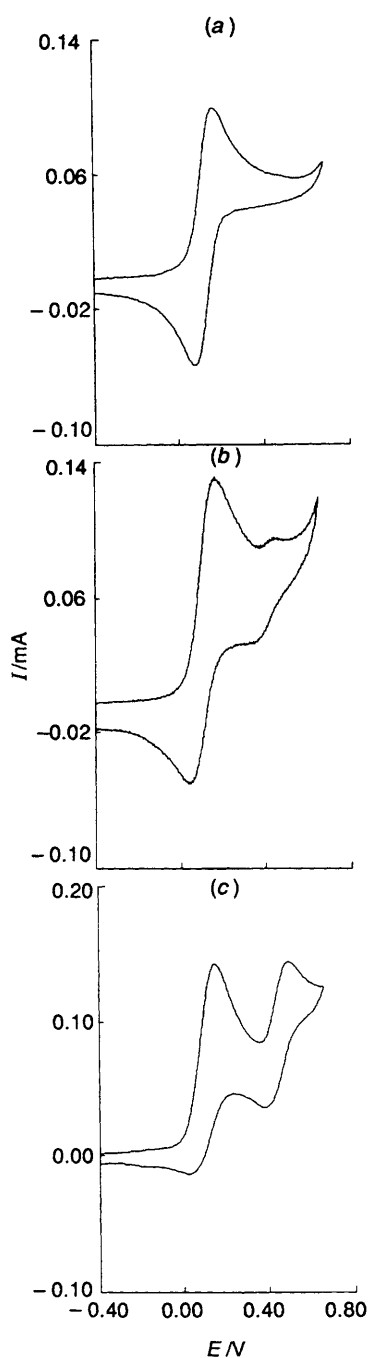The absence or presence of only a small peak at $E_{298}^{\ominus(2)}$ for

Fig. 12 Cyclic voltammetry of (a) [Co(OEtN$_3$C$_6$H$_3$Me$_2$-2,6)$_2$], (b) [Co(OMeN$_3$C$_6$H$_3$Me$_2$-2,6)$_2$] and (c) [Co(OEtN$_3$Ph)$_2$] in CH$_2$Cl$_2$ (5 × 10^{-3} mol dm^{-3}, 0.1 mol dm^{-3} NBu$_4$ClO$_4$) at platinum working electrode (scan rate 25 mV s^{-1}). Potentials are referenced vs. ferrocene–ferrocenium

Fig. 13 Least-squares plots of $E_{298}^{\diamond(1)}$ and $E_{298}^{\diamond(2)}$ vs. 2σ for [Co(OMeN$_3$-C$_6$H$_4$X-4)$_2$] chelates. X = OMe (a), Me (b), Et (c), H (d), Cl (e) and CO$_2$Et (f). ρ = 0.10 at $E_{298}^{\diamond(1)}$ and 0.26 at $E_{298}^{\diamond(2)}$. The values of σ are taken from ref. 15

cobalt(II) chelates with 2,6-Me$_2$, o-Me substituted phenyl rings or bulky R = Bu^t groups present in the ligand indicates that steric overcrowding prevents or at least restrains the high-potential oxidation process. This was shown in a series of spectroelectrochemical experiments. On coulometric oxidation of [Co(OEtN$_3$C$_6$H$_3$Me$_2$-2,6)$_2$] and [Co(OBu^{t}N$_3$C$_6$H$_4$Me-4)$_2$] at $E_{298}^{\diamond(1)}$ the initially brown solutions changed to deep green. The coulometric oxidations were simultaneously followed by electronic and ESR spectral methods. The electron spectra of the oxidised solutions reveal a characteristic transition at 15 300 (4000) and 12 400 cm^{-1} (ε = 3200 dm^3 mol^{-1} cm^{-1}) for the formed [Co(OEtN$_3$C$_6$H$_3$Me$_2$-2,6)$_2$]$^+$ and [Co(OBu^{t}N$_3$-C$_6$H$_4$Me-4)$_2$]$^+$ species respectively. With increasing Coulomb count the intensities of these bands, followed to a 0.90 e$^-$

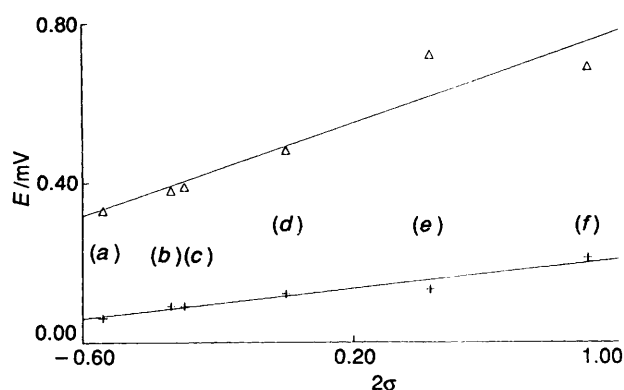transfer, increase linearly whereas the ESR spectra recorded at 77 K reveal a linear intensity decrease in characteristic signals[2m] due to the parent low-spin [Co(OEtN$_3$C$_6$H$_3$Me$_2$-2,6)$_2$] and [Co(OBu^{t}N$_3$C$_6$H$_4$Me-4)$_2$] chelates.

On coulometric oxidation of [Co(OEtN$_3$Ph)$_2$] at $E_{298}^{\diamond(1)}$ the initially brown solution turned first to red-violet and finally changed gradually to deep green on continuing the oxidation up to a coulometric count of 0.90 e$^-$, indicating, contrary to [Co(OEtN$_3$C$_6$H$_3$Me$_2$-2,6)$_2$] and [Co(OBu^{t}N$_3$C$_6$H$_4$Me-4)$_2$], the formation of an intermediate species. The electronic spectra show that with increasing coulometric count the intensities of the electronic transitions, characteristic for the red-violet intermediate species, observed at 13 200 (≈900) and 20 900 cm^{-1} (ε ≈1500 dm^3 mol^{-1} cm^{-1}) increase up to 0.5 e$^-$ and disappear gradually as the oxidation is continued to a 0.90 e$^-$ transfer. For the final deep green one-electron oxidation product [Co(OEtN$_3$Ph)$_2$]$^+$ a characteristic, intense electronic transition at 12 900 cm^{-1} (ε = 1600 dm^3 mol^{-1} cm^{-1}) is observed. In the ESR spectra the signal intensities of the low-spin form of [Co(OEtN$_3$Ph)$_2$]^{2m} decrease with increasing Coulomb count, but in contrast to what is observed for [Co(OEtN$_3$C$_6$H$_3$-Me$_2$-2,6)$_2$] and [Co(OBu^{t}N$_3$C$_6$H$_4$Me-4)$_2$] the sample became ESR silent at about 0.5 e$^-$ transfer. After addition of an equimolar amount of [Co(OEtN$_3$Ph)$_2$] to a solution of coulometrically prepared [Co(OEtN$_3$Ph)$_2$]$^+$ an electronic spectrum virtually identical with that of the red-violet intermediate species was observed.

In order to account for those observations the formation of a dimeric species, acting as the observed intermediate, according to equation (4) is postulated. The lack of any ESR signals due to

$$[Co^{II}L_2] + [Co^{III}L_2]^+ \rightleftharpoons [Co^{II}Co^{III}L_4]^+ \quad (4)$$
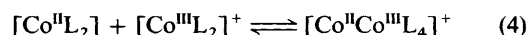
the low-spin form of the [Co^{II}L$_2$] chelate after a 0.5 e$^-$ transfer would be indicative for a short electron-spin relaxation time or fast spin exchange in the dimer. Within this model the second one-electron oxidation processes observed at $E_{298}^{\diamond(2)}$ would be related to the oxidation of the dimeric species [equation (5)]. As

$$[Co^{II}Co^{III}L_4]^+ \xrightarrow[+e]{-e} 2 [Co^{III}L_2]^+ \quad (5)$$
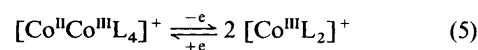
the ratios of peak currents $I_{pa}^{(1)}/I_{pa}^{(2)}$ and $I_{pc}^{(1)}/I_{pc}^{(2)}$ remain practically independent of the scan rate one may infer that the dimerisation process (4) is fast.

The proposed model was verified by coulometric studies followed by CV experiments. After completing a 0.5 e$^-$ transfer a CV curve was immediately recorded for a [Co(OEtN$_3$Ph)$_2$] sample. As shown in Fig. 14 the peak at 0.09 V disappeared almost completely whereas a peak at 0.41 V, corresponding to
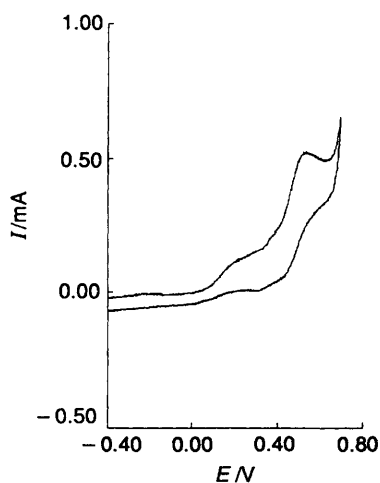
Fig. 14 Cyclic voltammogram for the sample from Fig. 12(c) after electrochemical oxidation (0.5 e^- transfer)

the oxidation of the postulated dimer, is clearly seen. The same is true of $[Co(OMeN_3C_6H_3Me_2-2,6)_2]$ which displays only a small peak at $E_{298}^{\theta(2)} = 0.40$ V. After a 0.5 e^- transfer was achieved the $I_{pa}^{(2)}/I_{pa}^{(1)}$ current ratio increased from 0.10 to 0.53, whereas $I_{pa}^{(2)}/I_{pa}^{(1)} = 0.2$ is to be expected if the formed $[Co(OMeN_3C_6H_3Me_2-2,6)_2]^+$ species does not contribute to the formation of a species electrochemically active in the $E_{298}^{\theta(2)}$ potential range. On the basis of the above results the mechanisms proposed in (4) and (5) seem plausible.

Conclusion

The results obtained have shown that triazene 1-oxides present a unique, significantly differing from typical bidentate Schiff bases, class of N,O-donor ligands stabilising the low-spin state of their cobalt(II) bis(chelates) in the solid state. The stereoelectronic properties of these ligands can be varied widely and allowed the first isolation of the high- and low-spin isomers of cobalt(II) bis(chelates) or their conglomerates. In non-coordinating solvents the high spin–low spin equilibria related to square planar–tetrahedral interconversions are observed.

The complexes studied reveal a pronounced dependence of the structure (and hence the spin state) and the electrochemical properties on the ligand substituents. The same effect has been previously found in the reactivity of their Lewis-base adducts towards dioxygen.[2k] The ligand substituents may influence the electronic properties either due to their polar effect (*para* substituents) or, indirectly, by controlling the conformation of the ligand (*ortho* substituents). Furthermore, the size of the R groups and the presence of *o*-methyl groups seemingly control the possibility of intermolecular interactions. The latter effect is reflected by the strong sensitivity of the structure in the solid state and the formation of intermediate dimeric products upon electrochemical oxidation to the above details of the ligand structure.

Acknowledgements

References

1 M. Elkins and L. Hunter, *J. Chem. Soc.*, 1938, 1346.

2 (a) R. L. Dutta and R. Sharma, *J. Sci. Ind. Res.*, 1981, **40**, 715 and refs. therein; (b) D. J. Hodgson, *Inorg. Chim. Acta*, 1983, **75**, 225; (c) M. V.

Rajasekharan, K. I. Varughese and P. T. Manoharan, *Inorg. Chem.*, 1979, **18**, 2221; (d) M. F. Rudolf, *Bull. Pol. Acad. Sci., Chem.*, 1979, **27**, 747; (e) S. Bhattacharya, A. Chakravorty, F. A. Cotton and W. Schwotzer, *Inorg. Chem.*, 1984, **23**, 1709; (f) D. Ray, S. Pal and A. Chakravorty, *Inorg. Chem.*, 1986, **25**, 2676; (g) R. Mukherjee, O. A. Rajan and A. Chakravorty, *Inorg. Chem.*, 1982, **21**, 785; (h) R. Mukherjee and A. Chakravorty, *J. Chem. Soc., Dalton Trans.*, 1983, 955; (i) R. Mukherjee and A. Chakravorty, *J. Chem. Soc., Dalton Trans.*, 1983, 2197; (j) M. F. Rudolf, J. A. Wolny, Z. Ciunik and P. Chmielewski, *J. Chem. Soc., Chem. Commun.*, 1988, 1006; (k) M. F. Rudolf, J. A. Wolny, T. Lis and P. Starynowicz, *J. Chem. Soc., Dalton Trans.*, 1992, 2079; (l) Z. Ciunik, J. A. Wolny and M. F. Rudolf, *Acta Crystallogr., Sect. C*, 1991, **47**, 2539; (m) M. F. Rudolf, J. A. Wolny, J. Baranowski and M. Kolbuszewski, *Polyhedron*, 1992, **17**, 2129; (n) M. F. Rudolf, Z. Ciunik, K. Gatner and J. A. Wolny, *Polyhedron*, 1992, **11**, 2591; (o) D. N. Purohit, *Spectrochim. Acta, Part A*, 1985, **41**, 873; (p) P. S. Zacharias and A. Ramachandraiah, *Polyhedron*, 1985, **4**, 1013; (q) G. L. Dwivedi and R. C. Srivastava, *Acta Crystallogr., Sect. B*, 1971, **27**, 2316; (r) G. L. Dwivedi and R. C. Srivastava, *Acta Crystallogr., Sect. B*, 1976, **32**, 1446; (s) J. M. Elizabathe and P. S. Zacharias, *Indian J. Chem., Sect. A*, 1989, **28**, 1064.

3 (a) R. Holm and M. J. O'Connor, *Prog. Inorg. Chem.*, 1971, **14**, 241 and refs. therein; (b) T. Frömmel, W. Peters, H. Wünderlich and W. Kuchen, *Angew. Chem., Int. Ed. Engl.*, 1992, **5**, 612; (c) A. Deeg, W. Kuchen, D. Langsch, D. Mootz, W. Peters and H. Wünderlich, *Z. Anorg. Allg. Chem.*, 1991, **606**, 119; (d) M. Fuchs, W. Kuchen and W. Peters, *Chem. Ber.*, 1986, **119**, 1569; (e) D. Langsch, Ph.D. Thesis, Düsseldorf, 1989.

4 G. W. Everett and R. H. Holm, *Inorg. Chem.*, 1968, **7**, 776; *J. Am. Chem. Soc.*, 1966, **88**, 2442; D. H. Gerlach and R. H. Holm, *Inorg. Chem.*, 1969, **8**, 2292.

5 D. F. Evans, *J. Chem. Soc.*, 1959, 2003; S. K. Sur, *J. Magn. Reson.*, 1989, **82**, 169.

6 *Techniques of Organic Chemistry*, Interscience, New York, London, 1955, vol. 7.

7 H. Beckmann, *Liebigs Ann. Chem.*, 1906, **365**, 204.

8 *Methoden der Organischen Chemie (Houben-Weyl)*, Georg Thieme Verlag, Stuttgart, 1963, vol. X/3.

9 E. Bamberger and E. Renauld, *Chem. Ber.*, 1896, 2396.

10 N. Walker and D. Stuart, *Acta Crystallogr., Sect. A*, 1983, **39**, 158.

11 Syntex XTL/XTLE Structure Determination System, Syntex Analytical Instruments, Cupertino, 1976.

12 G. M. Sheldrick, *Acta Crystallogr., Sect. A*, 1990, **46**, 467.

13 G. M. Sheldrick, SHELX 76, Program for Crystal Structure Determination, University of Cambridge, 1976.

14 *International Tables for X-Ray Crystallography*, Kynoch Press, Birmingham, 1974, vol. 4.

15 R. A. Y. Jones, *Physical and Mechanistic Organic Chemistry*, Cambridge University Press, Cambridge, 1979.

16 P. S. Zacharias and A. Chakravorty, *Inorg. Chim. Acta*, 1972, **6**, 623.

17 V. P. Chacko and P. T. Manoharan, *J. Magn. Reson.*, 1974, **16**, 75; 1976, **22**, 7.

18 C. K. Johnson, ORTEP II, Report ORNL 5138, Oak Ridge National Laboratory, Oak Ridge, TN, 1976.

19 M. A. Hitchman, *Inorg. Chem.*, 1982, **21**, 821.

20 E. König, *Prog. Inorg. Chem.*, 1987, **35**, 527.

21 (a) M. Mikami, M. Konno and Y. Saito, *Chem. Phys. Lett.*, 1979, **63**, 566; (b) B. A. Katz and C. K. Strouse, *J. Am. Chem. Soc.*, 1979, **101**, 6214.

22 R. D. Shannon and C. T. Prewitt, *Acta Crystallogr., Sect. B*, 1969, **25**, 929.

23 M. Calligaris, D. Minichelli, G. Nardin and L. Randaccio, *J. Chem. Soc. A*, 1970, 2411.

24 M. Calligaris, G. Nardin and L. Randaccio, *J. Chem. Soc., Dalton Trans.*, 1974, 1903.

25 P. Thuéry, J. Zarembowitch, A. Michalowicz and O. Kahn, *Inorg. Chem.*, 1987, **26**, 851.

26 J. Gažo, I. B. Bersuker, J. Garaj, J. Kohout, M. Kabešowa, H. Langfeldowa, M. Melnik, M. Serator and F. Valach, *Coord. Chem. Rev.*, 1976, **19**, 253.

27 E. König, G. Ritter and S. K. Kulshreshta, *Chem. Rev.*, 1985, **85**, 219.

28 J. March, *Advanced Organic Chemistry: Reactions, Mechanisms and Structure*, Wiley, New York, 1985.

29 M. F. Rudolf, Z. Ciunik, K. Drabent and J. A. Wolny, *J. Chem. Soc., Perkin Trans. 2*, submitted for publication.